表　日本人集団における各遺伝リスクの大きさ（寄与度）

	遺伝リスクマーカー	日本人集団におけるリスクアレル頻度	オッズ比	人口寄与危険度（もしこのリスクが、日本人集団になかったら、何%の患者が減るか）
PARK16	rs947211	0.50	1.30	13.0
BST1	rs11931532	0.42	1.24	9.1
SNCA	rs11931074	0.58	1.37	17.6
LRRK2	rs1994090	0.08	1.39	3.0
Tau	rs393152	1.00	1.30	23.0
GBA	RecNcil	0.0018	7.21	1.1（*GBA*内の11個の変異を全てたし合わせると、4.6）

人口リスク寄与度（もしこのリスクが日本人集団になかったら，何%の患者が減るかの指標）を示す。SNPはオッズ比は低いが人口リスク寄与度は高い。GBAなどのrare variantはその逆である。

を明示した。原因変異により常染色体優性遺伝性PDを引き起こす遺伝子が，そのSNPを通して，孤発性PDの遺伝リスクとなったことは興味深い。このような関係は，PDを超えて，ほかの疾患に対しても，あてはまると思われる[2]。

*PARK16*領域には，3つの遺伝子が存在するが，発現量的形質座解析から，*NUCKS1*が，最も有力な責任遺伝子であると考えた（図1a）。*NUCKS1*は，リン酸化部位をふくむ核タンパクであるが，神経系における機能は，未知であり，新たなPD発症のパスウェイを開拓する可能性がある[8]。

*BST1*は，細胞内Ca^{2+}貯蔵からのCa^{2+}放出を誘発するサイクリックADPリボースの形成を触媒する酵素であり[9]，最近提唱されている，ドパミン細胞死のCa^{2+}ストレス説を想起させ，興味深い。これらは従来のPD病態説からは全く新規な遺伝子であり，従来説にとらわれず，新規なものを同定できるところにGWASの強みがある。

さらに最近アメリカの別グループのGWASから，HLA-DR抗原の領域との関連が報告された（$P = 1.9 \times 10^{-10}$）。PD脳ではDR抗原陽性のミクログリアが検出されること，NSAIDSは疫学的にPDのリスクを減少させることなどもあり，PDと炎症の関係を示しており興味深い[10]。

3. 第二世代のGWAS

さらにパーキンソン病においては，さらなる国際共同研究として欧米の５つのグループがそれぞれ独立に行っていたGWASを合わせてメタ解析を行い（計患者5333，対照12019），有意なSNPをさらに患者7053，対照9007で再現実験を行い，ゲノムワイド有意水準$P < 5\times$

10^{-8}を超える遺伝子を従来の6個の他に，*ACMSD*, *STK39*, *LAMP3*, *SYT11*, *CCDC62*の5個を同定した[11]。

GWASによって多数の疾患感受性遺伝子が同定されたものの，それらは遺伝要因全体の一部しか説明できないことから（missing heritability），SNPとしては，このような圧倒的な数の試料を各地から集めてゲノムワイドメタ解析を行いより多くの感受性遺伝子を同定することが行われだしており，「第2世代のGWAS」とも言われている。

おわりに

おそらく数10個あるパーキンソン病の疾患感受性遺伝子としては，αシヌクレイン，GBA，今回のPARK16，BST1，LRRK2など以外に確立されたものは少ないのが現状であり，今後のGWASからさらなる遺伝子の解明，そこから新たな疾患パスウェイとそこからの治療薬開発が期待される（図2）。これら4座位（1q32, 4p15, 4q22, 12q12）の，人口リスク寄与度（もしこのリスクが日本人集団になかったら，何%の患者が減るかの指標）を示すが，それぞれ13%, 8%, 18%, 3%と見積もられ，SNPはオッズ比は低いが人口リスク寄与度は高い。GBAなどのrare variantはその逆であり，どちらも重要である（表）[2]。

しかし現在のSNPチップによるGWASでは，アレル頻度の低いものは同定不可能であり（搭載されていない），rare variantは見過ごされてしまう。エクソンキャプチャー，次世代シークエンサーによるエキソームリシークエンスが行われており，期待される。

文献

1) Farrer MJ : Genetics of Parkinson disease: paradigm shifts and future prospects. Nat Rev Genet 7:306-318, 2006.
2) Satake W, *et al*: Genome-wide association study identifies common variants at four loci as genetic risk factors for Parkinson's disease. Nat Genet 41:1303-1307, 2009.
3) Mueller JC, *et al*: Multiple regions of alpha-synuclein are associated with Parkinson's disease. Ann Neurol 57: 535-541, 2005.
4) Mizuta I, *et al*: Multiple candidate gene analysis identifies a-synuclein as a susceptibility gene for sporadic Parkinson's disease. Hum Mol Genet 15:1151-1158, 2006.
5) Mitsui J, *et al*: Mutations for Gaucher disease confer a high susceptibility to Parkinson disease. Arch Neurol 66:571-576, 2009.
6) Sidransky E, *et al*: Multicenter analysis of glucocerebrosidase mutations in Parkinson's disease. N Engl J Med 361: 1651-1661, 2009.
7) Simon-Sanchez J, *et al*: Genome-wide association study reveals genetic risk underlying Parkinson's disease. Nat Genet 41: 1308-1312, 2009.
8) Ostvold AC, *et al*: Molecular cloning of a mammalian nuclear phosphoprotein NUCKS, which serves as a substrate for Cdk1 *in vivo*. Eur J Biochem 268: 2430-2440, 2001.
9) Yamamoto-Katayama S, *et al*: Crystallographic studies on human BST-1/CD157 with ADP-ribosyl cyclase and NAD glycohydrolase activities. J Mol Biol 316: 711-723, 2002.
10) Hamza TH, *et al*: Common genetic variation in the HLA region is associated with late-onset sporadic Parkinson's disease. Nat Genet 42:781-785, 2010.
11) International Parkinson Disease Genomics Consortium: Imputation of sequence variants for identification of genetic risks for Parkinson's disease: a meta-analysis of genome-wide association studies. Lancet 377:641-649, 2011.

＜Special Article＞
孤発性パーキンソン病の分子病態機序はどこまで解明されたか

戸田達史*

要旨

- 孤発性パーキンソン病の発症機序としては，ミトコンドリア呼吸系酵素の障害，炎症反応，酸化ストレス障害が一因とされてきたが，遺伝性パーキンソン病家系の解析などから6つのメンデル遺伝性原因遺伝子が明らかにされ，蛋白分解異常の重要性が示された．
- ゲノムワイド関連解析による新たな疾患感受性遺伝子の同定や，ゴーシェ病変異もrare variantとして重要である．
- α-シヌクレインのミスフォールド蛋白質が近隣の神経細胞に伝播していくシヌクレインプリオン仮説も提唱されている．
- ミクログリアの活性化を伴う継続的な炎症状態も注目される．

はじめに

パーキンソン病(PD)は，臨床的には，振戦，筋固縮，寡動，姿勢反射障害を主徴とし，認知症，自律神経障害などのさまざまな随伴症状を呈する神経変性疾患である．わが国には16万人以上の患者が存在するが，今後社会の高齢化に伴いさらなる患者数増加が予想されている．一部は遺伝性であるが，患者の約95%は孤発性であり，本稿では孤発性PDの分子病態機序について，現在主流となっている仮説に加え，最近のトピックスも含めて概観する．

孤発性PDは多因子遺伝性疾患である

症例的には大多数(90%以上)の孤発性PDの原因は，現時点では不明であるが，加齢および複数の影響力の弱い遺伝因子(おそらく数十個からなる)と環境要因の組み合せにより発症する多因子遺伝性疾患と考えられている．Fig. 1に示すように各遺伝要因と環境要因の総和が閾値を超えたときに発症すると考えられている(Fig. 1)．遺伝要因が関係するということの根拠は，①患者の約10%に家族内発症がみられる，②患者の同胞における有病率の一般集団の有病率に対する比(λs)は6.7(アイスランドの報告)，③一卵性双生児での疾患一致率(55%)が二卵生双生児での一致率(18%)の約3倍であった，ということから示唆されている．

一方，PD症例の90%以上は孤発性発症であるが，5～10%は家族性(その一部はメンデル遺伝性)に発症する．メンデル遺伝性PD家系の連鎖解析などから，6つのメンデル遺伝性PD原因遺伝子(*α-シヌクレイン*，*パーキン*，*LRRK2*遺伝子

* T. Toda(教授)：神戸大学大学院医学研究科神経内科学．

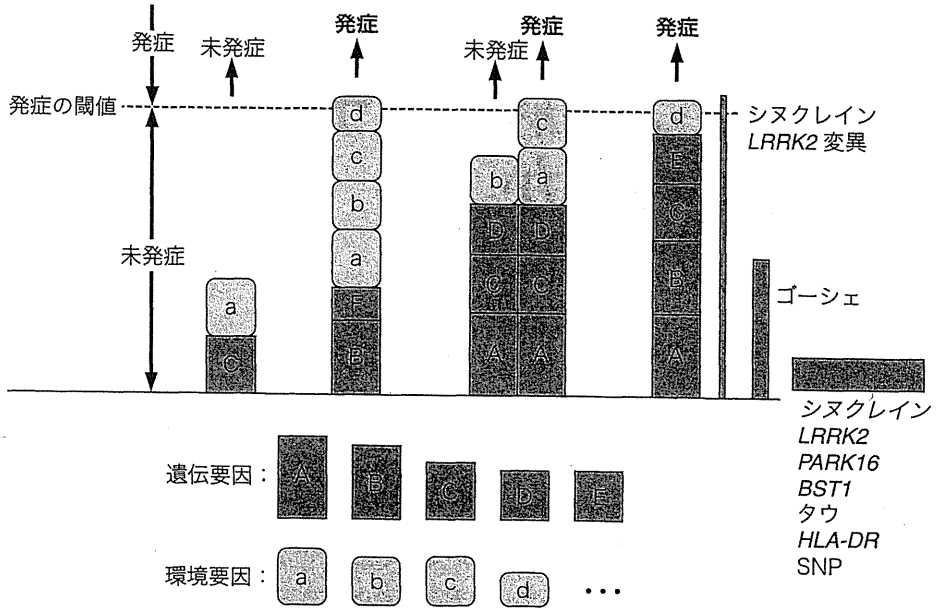

Fig. 1. 孤発性 PD は多因子遺伝性疾患

PD，アルツハイマー病，または生活習慣病を含むほとんどの疾患は，複数の遺伝要因と複数の環境要因の積み木の総和が，ある閾値を超えたとき発症すると考えられている．メンデル遺伝性変異以外に，common variant として *α*-シヌクレイン，*PARK16*，*BST1*，*LRRK2*，タウ，*HLA-DR* の SNP が，また rare variant としてゴーシェ病遺伝子が重要である．

など)が明らかにされた．これまでにレビー小体の主要構成成分である *α*-シヌクレインのほか，プロテアソーム系に関係する遺伝子(パーキン，*UCH-L1*)，ミトコンドリアに関係する遺伝子(*PINK1*，*DJ-1*)，酸化ストレスに関係する遺伝子(*DJ-1*)などが同定されている．孤発性 PD，メンデル遺伝性 PD とも，一部共通の発症メカニズムが存在していると考えられ，それらを切り口にして孤発性 PD の病態解明が進んでいる[1]．

メンデル遺伝性 *PARK* 遺伝子の孤発性 PD 病態における立ち位置

1）*PARK1*，*PARK4*(*α*-シヌクレイン)について→1997 年に *PARK1*(*α*-シヌクレイン)遺伝子が同定されたのを皮切りに，次々に *PARK* 遺伝子の同定が進むと，そのほとんどが孤発性 PD の病態メカニズムにも関係する蛋白であることが判明した(Table 1，Fig. 2)[1]．もっともインパクトが強かったのは，*PARK1* 遺伝子産物 *α*-シヌクレイン蛋白が，メンデル遺伝性 PD，孤発性 PD 両方のレビー小体の主要成分であったという報告である．*α*-シヌクレインはメンデル遺伝性 PD，孤発性 PD の病態に共通した分子であることにより，*α*-シヌクレイン変異の解析は，孤発性 PD のモデルにもなると考えられる．アミノ酸変異をもつ *α*-シヌクレインは *in vitro* で重合化が促進することが知られており，野生型 *α*-シヌクレイン蛋白もリン酸化やニトロ化を受けて患者脳で蓄積していることが報告されている[2]．また，*PARK4* が，野生型 *α*-シヌクレインを含む 1.6〜2.0 Mb の三重重複であったことが報告され，正常 *α*-シヌクレインの mRNA，蛋白発現レベルが増加すれば発症にいたることが示された．

現在，*α*-シヌクレイン蛋白は生理的には可溶性単量体(monomer)として存在し，特定の構造をとらないが，種々の要因で重合化，不溶化，凝集する過程で何らかの神経毒性をもたらすと考えられている．そして，孤発例では，*α*-シヌクレインの

Table 1. 孤発性 PD の機序に関する主な仮説とエビデンス

機　序	エビデンス
ミトコンドリア機能障害	患者にミトコンドリア機能低下 パーキンソン様症状を起こす神経毒(MPTP，rotenone など)はミトコンドリア機能を障害 ミトコンドリア機能に関係する遺伝子がメンデル遺伝型家系で同定(*PINK1*，*DJ-1* など)
プロテアソーム機能低下	プロテアソーム機能に関係する遺伝子がメンデル遺伝型家系で同定(パーキン，*UCH-L1* など) PD 動物モデルでプロテアソーム活性低下
酸化ストレス	患者で酸化ストレスマーカーの増加 パーキンソン様症状を起こす神経毒(MPTP, rotenone, 6-OHDA など)の作用過程でフリーラジカル産生 メンデル遺伝型家系遺伝子の 1 つ *DJ-1* は酸化ストレス防御作用
α-シヌクレイン蓄積	レビー小体の主成分は α-シヌクレイン メンデル遺伝型家系でみられるアミノ酸変異をもつ合成蛋白の凝集性促進 メンデル遺伝型の正常 α-シヌクレイン遺伝子重複家系で，蛋白・遺伝子発現レベルが上昇 培養細胞，動物モデルで，封入体を伴った神経細胞死

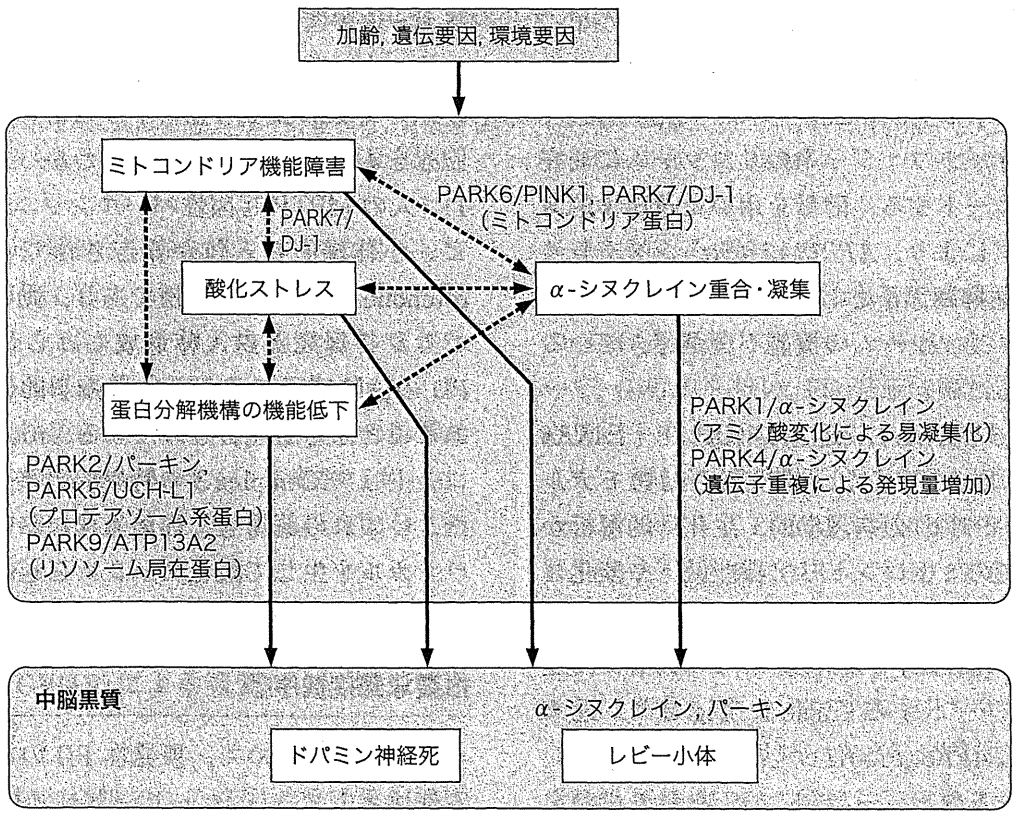

Fig. 2. 孤発性 PD 発症機序と *PARK* 遺伝子

重合が促進されるような，変異以外の要因が働いて，発症にいたると考えられている[3]．その際にはα-シヌクレインが小胞体-ゴルジ体の小胞輸送を障害し，神経変性を起こすことが報告されている[4]．

2）*PARK2*(パーキン)，*PARK9*(*ATP13A2*)について→孤発性 PD の病理では，レビー小体がユビキチン抗体で染まる，脳でオートファジーの亢進がみられる，という報告がある．このことと，蛋白分解機構に関する *PARK* 遺伝子の存在によ

り，プロテアソーム系，オートファジー系の蛋白分解機構の破綻がPDの病態に関係するという仮説がたてられた(Table 1，Fig. 2)[5,6]．*PARK2*(パーキン)蛋白の機能については，ユビキチン・プロテアソーム系蛋白分解において，基質にユビキチンを結合させるE3ユビキチンリガーゼであることが明らかにされた．ユビキチンリガーゼはプロテアソームにより分解を受けるべき蛋白質にユビキチンという目印をつける酵素であり，ユビキチン・プロテアソーム系の破綻によって本来分解される蛋白質(すなわちパーキンの基質)が蓄積することで神経変性を引き起こしていると考えられている．このパーキンの基質はさまざまな報告があるが，真の基質はどれであるか結論が出ていない．

PARK9(*ATP13A2*)は近年発見され，進行が早く核上性上方注視麻痺を呈するなど非典型的である．原因遺伝子はlysosomal type 5 P-type ATPaseと呼ばれ，オートファジー系のリソソームに局在する蛋白をコードする．酵母を用いた遺伝学的スクリーニングにより，*ATP13A2*がα-シヌクレインの細胞毒性抑制因子として同定された[7]．劣性遺伝であり，リソソームの機能不全が起きていると考えられる．

3）*PARK6*(*PINK1*)，*PARK7*(*DJ-1*)，*PARK8*(*LRRK2*)について→また，剖検脳や動物モデル(薬物性PDモデル)の病理学的・生化学的解析から，孤発例でのミトコンドリア機能低下や酸化ストレスマーカーの増加が報告されていた．*PARK6*(*PINK1*)，*PARK7*(*DJ-1*)は，これらの機構に関連する蛋白をコードする(Table 1，Fig. 2)[8]．近年パーキンと*PARK6*(*PINK1*)が共同してミトコンドリアのオートファジー(ミトファジー)の役割を担うことが明らかにされ，変異があると機能低下した異常ミトコンドリアの除去ができなくなると考えられる[9]．*PARK7*の原因はDJ-1蛋白であり，ミトコンドリアに移行し抗酸化作用をもちドパミン細胞死との関係が注目される．また*PARK8*は常染色体優性遺伝形式を呈するものの中で最多であり，原因蛋白はLRRK2というキナーゼであり，疾患型変異はキナーゼ活性の亢進をもたらすことから，そのリン酸化基質がPDにおいて重要な役割を担うと考えられる．シヌクレインに対するキナーゼ活性が注目されているが定かではない．

神経毒の解析

PDの症状を引き起こす薬物として，MPTP(1-methyl-4-phenyl-1,2,3,6-tetrahydropyridine)，ロテノン(rotenone)，6-OHDAなどが知られており，これらの作用機序からも，病態を考察することができる．これらの神経毒のうち，病理学的にも孤発性PDと類似する所見を示すのが，MPTPとrotenoneである．MPTPは麻薬の合成過程の副産物であり，脳内でMPP^+となりドパミントランスポーターを介してドパミン神経に取り込まれ，エネルギー産生の場であるミトコンドリア電子伝達系のComplex Iを阻害することにより，神経細胞死をもたらすということがわかっている(Table 1)．人のMPTP起因性パーキンソニズムでは，レビー小体様の封入体が報告されている．また，rotenoneは，農薬の一種であり，動物モデルでドパミン神経死と封入体形成がみられる．農薬がPDの危険因子であるという疫学的研究の報告があることからも注目されている．rotenoneもミトコンドリアComplex Iの特異的阻害薬である．また，いずれの薬物も，作用過程において，フリーラジカルを生じて酸化ストレスを起こすことも知られている(Table 1)．

主要な発症機序

これらをまとめて，孤発性PDの神経死にいたる機序として，①ミトコンドリア機能障害により，細胞内エネルギー産生が低下する，②蛋白分解機構(プロテアソーム系，オートファジー系など)機能低下により，神経細胞内に構造異常をきたした蛋白が貯まって，細胞毒性をもつ，③酸化ストレス(活性酸素物質：reactive oxygen spieces(ROS))が細胞毒性をもつ，などがさまざまな割合で関与していること，そして④α-シヌクレイン

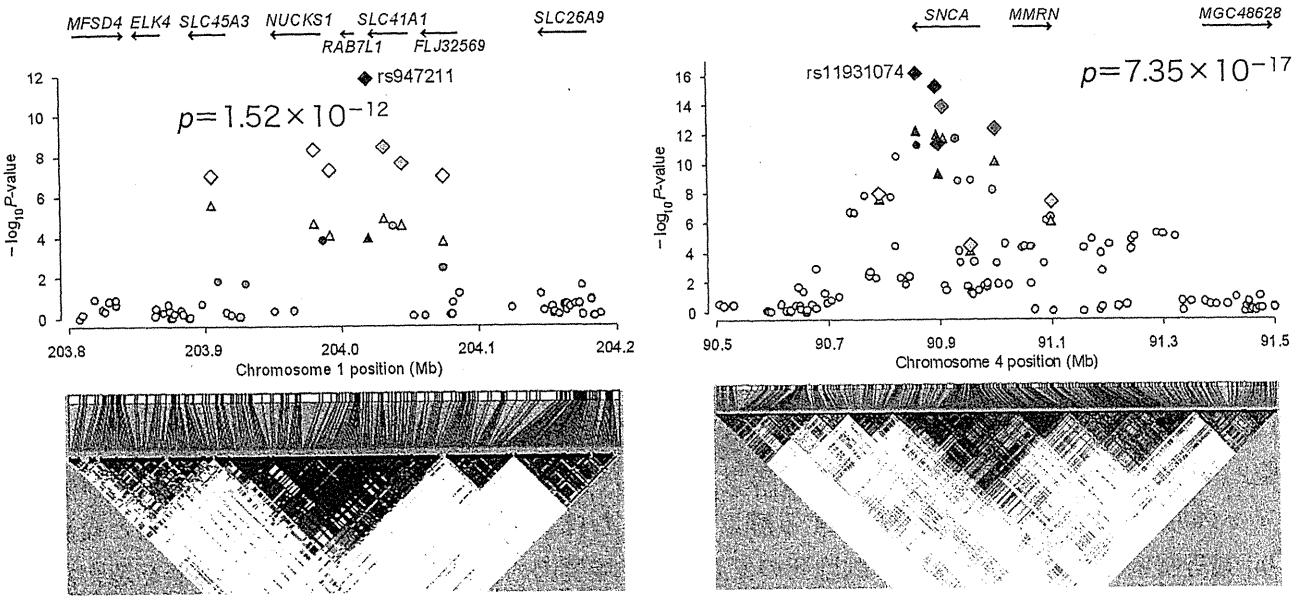

a．*PARK16*(1q32)　　b．α-シヌクレイン(4q22)

Fig. 3. 日本人 PD 患者 2011 検体，対照 18381 検体のゲノムワイド関連解析より同定された 4 つの PD 遺伝子座の抜粋

このうち 2 つはまったく新規の領域であった．とくに(a)は非常に強い関連を示し，白人集団でも関連が再現されたことから *PARK16* と名づけた．また残りの 2 つは，常染色体優性遺伝性パーキンソニズムの原因遺伝子 α-シヌクレイン(b)と *LRRK2* を含む領域が同定された．縦軸は-logP，すなわち上にいくほど関連が強い．［文献 10)より引用］

蛋白がこれらの経路あるいは別の経路に関与していることについては，あまり異論がない．さらに各機序の関与を裏づける報告も剖検脳の病理学的・生化学的解析から得られている(Table 1)．これらの機序は複数の遺伝要因や環境要因の影響のもとで，それぞれ，あるいは互いに影響しあって，孤発性 PD の病態を形成していくと現在のところ考えられている(Fig. 2)．

ゲノムワイド関連解析(Genomewide Association Study：GWAS)による孤発性 PD 感受性遺伝子の同定◎

ここ 10 年間孤発性 PD の疾患感受性遺伝子の発見を目指した多くの研究がなされてきたが，アルツハイマー病における ApoE4 多型のような確実に発症リスクを高める遺伝因子はなかなか確認されていなかった．ゲノムワイド有意水準($p<5\times10^{-8}$)を満たす確実なものは，α-シヌクレインの 3′非翻訳領域 SNP(Gasser ら，筆者らが同定)とゴーシェ病遺伝子 *GBA* の rare variant の 2 つの遺伝子のみであった．

われわれは，大規模の患者対照集団と，56 万個の SNP を搭載したイルミナ Hap550 アレイを用いて，GWAS を行い，PD 発症に関わる 2 つの新しい遺伝子座 *PARK16*，*BST1* を同定した(Fig. 3a)．また，常染色体優性遺伝性 PD の原因遺伝子 α-シヌクレイン，*LRRK2* の弧発性 PD への関与を証明した(Fig. 3b)．白人の PD の GWAS 研究を行っていたグループと共同し，α-シヌクレイン・*PARK16*・*LRRK2* は 2 人種に共通の PD リスクであり，タウ・*BST1* のリスク多型の影響は人種特異的であることを示した[10]．

また孤発性 PD の発症に，常染色体優性遺伝性 PD の原因遺伝子が密に関係していることを示した．原因変異により常染色体優性遺伝性 PD を引き起こす遺伝子が，その SNP を通して，孤発性 PD の遺伝リスクとなったことは興味深い．すなわち，α-シヌクレイン，*LRRK2* が関与する病理経路が，孤発性を含めた PD 全体の病因の根幹をなすことを示している．一方，微小管の安定化に

働くタウは，アルツハイマー病，前頭側頭型認知症などの原因産物として知られており，PDと他神経変性疾患との共通の病理経路の存在をも示唆している[10]．

PARK16 領域には，3つの遺伝子が存在するが，発現量的形質座解析から，*NUCKS1* が，もっとも有力な責任遺伝子であると考えた(Fig. 3a)．*NUCKS1* は，リン酸化部位を含む核蛋白であるが，神経系における機能は，未知であり，新たなPD発症病態を開拓する可能性がある．*BST1* は，細胞内 Ca^{2+} 貯蔵からの Ca^{2+} 放出を誘発するサイクリックADPリボースの形成を触媒する酵素であり，最近提唱されているドパミン細胞死の Ca^{2+} ストレス説を想起させ，興味深い．これらは従来のPD病態説からはまったく新規な遺伝子であり，従来説にとらわれず，新規なものを同定できるところにGWASの強みがある．

さらに最近別グループのGWASから，HLA-DR抗原の領域との関連が報告された．PD脳ではDR抗原陽性のミクログリア(後述)が検出されること，非ステロイド抗炎症薬(NSAIDs)は疫学的にPDのリスクを減少させることなどもあり，PDと炎症の関係を示しており興味深い[11]．

PDとゴーシェ病とまれな多型(rare variant)

リピドーシスの常染色体劣性遺伝のユダヤ人ゴーシェ病家系内にPD患者が多いことから，PDでは *GBA*(glucocerebrosidase，1q21)変異のヘテロ保因者が有意に多いことが報告された[12]．東京大学神経内科とわれわれの共同研究グループは，*GBA* 遺伝子の全11エクソンとその近傍をPD患者534人，対照544人リシーケンスして塩基配列変化の有無を調べ，11種類の疾患原性点変異が同定された．ヘテロでもつ保因者はPD患者534人中50人(9.4%)，対照544人中2人(0.37%)であり，PDと *GBA* 変異は強く関連していた($p = 6.9\times10^{-14}$，オッズ比28.0)[12]．

さらに全世界での米国人，フランス人，ポルトガル人，台湾人など計約10,000人の患者対照集団のメタ解析により，どの人種にても *GBA* 遺伝子はリスクとなり平均オッズ比は5である[13]．*GBA* 変異は確実なPDリスク因子であり，SNPによるCommon Disease-Common Variants 仮説と異なり，Common Disease-Multiple Rare Variant 仮説によるものである．すなわち，頻度は低いが発症へのeffect sizeが大きい．なぜリスクとなるかの原因は不明であるが，単なる酵素活性低下でなく，*GBA* 変異の蛋白分解機構への負担によることも推定されている．

PD，アルツハイマー病，または生活習慣病を含むほとんどの疾患は，複数の遺伝要因と複数の環境要因の積み木の総和が，ある閾値を超えたとき発症すると考えられている．これまでみてきたように *α-シヌクレイン* や *LRRK2* の変異はそれ1つだけで閾値に到達し発症するが，対象患者はほとんど存在しないので積み木の幅はとても狭い．ゴーシェ病遺伝子などのrare variantは中等度の高さをもつが10%以下の患者にしか当てはまらないため幅は狭い．一方SNPは，それ自体のオッズは低いがほとんどの患者に当てはまるため，積み木の幅は広い．いずれも重要である(Fig. 1)．

シヌクレインプリオン仮説

本特集別稿を参照されたいが，Braakらはα-シヌクレインの蓄積部位を多数例のPD脳で詳細に検討し，この蛋白質の異常蓄積はまず嗅球，延髄から始まり，徐々に上行して橋，中脳に及び，最終的に大脳皮質にいたるという仮説を提唱し，Braak仮説として有名である．

一方，PDの治療を目的として胎児の中脳腹側組織を移植し10年以上経過した患者脳を病理学的に検索したところ，驚くべきことに移植された神経細胞にレビー小体が認められた[14]．またα-シヌクレインを高発現する神経細胞とマウスの幹細胞を共培養する *in vitro* 実験や，α-シヌクレインを発現するトランスジェニックマウスの海馬に幹細胞を移植する *in vivo* 実験にて，いずれの場合にも幹細胞の細胞質にα-シヌクレインの凝集体が

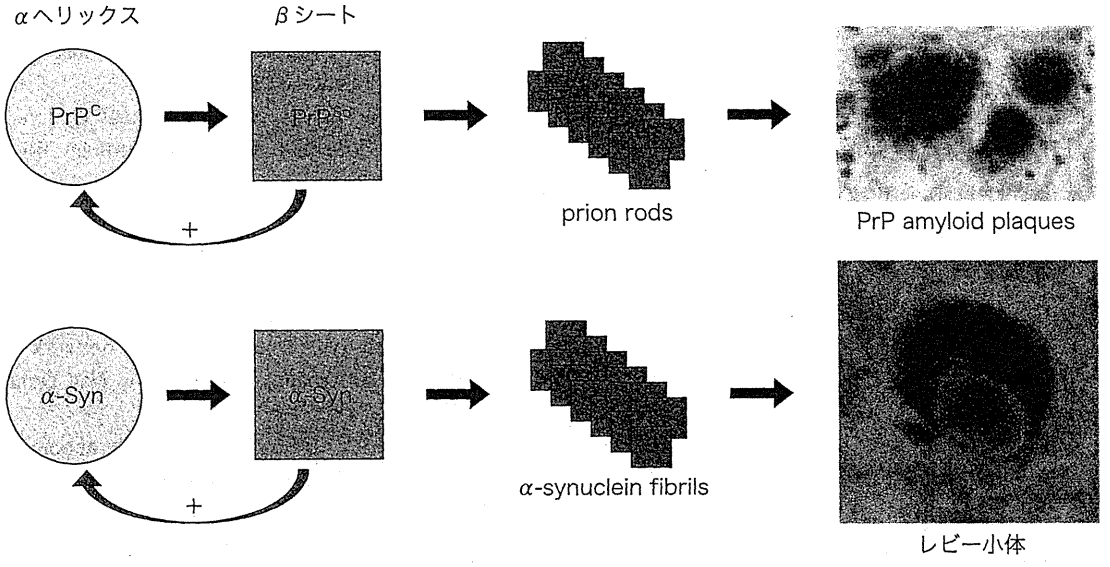

未知の環境要因→嗅覚器や腸管(外界)→自律神経叢や嗅球でα-シヌクレインのミスフォールディング→放出伝播？

Fig. 4. PD のシヌクレインプリオンモデル

[文献 16)より引用]

形成されること，α-シヌクレインがエンドサイトーシスによって幹細胞に取り込まれることが示された．これらの知見は，α-シヌクレインが近接する神経細胞に「伝染」する可能性を示している．またごく最近，細胞内のα-シヌクレインが，他の細胞に移動し凝集し，その凝集体の量が継時的に増加すること，α-シヌクレイン蛋白の細胞内取り込みに関してエンドサイトーシス阻害薬の同時注入により，取り込みの減少が明らかとなった[15]．

α-シヌクレインもプリオン蛋白質と同様に，αヘリックス構造とβシート構造をとりうることから，何らかのきっかけでβシート化したα-シヌクレインがシードとなって凝集を開始するとともに，細胞外に放出されて近隣の細胞に取り込まれ，プリオン病と同様の機序で病変が進展するという，PD のプリオンモデルが提唱されている(Fig. 4)．さらにこのモデルと Braak 仮説を合わせて PD の発症機序として，未知の環境要因が嗅覚器や腸管など外界に接した神経組織に作用し，自律神経叢や嗅球において最初にα-シヌクレインのミスフォールド蛋白質が形成され，逆行性に細胞体まで輸送され，中枢神経内で放出されて近隣の神経細胞に連続的に伝播していく，という大胆な仮説もある(Fig. 4)[16]．中枢神経内におけるα-シヌクレインの伝播を防ぐことで(例：エンドサイトーシス阻害薬)PD の進行を抑制するという，新たな治療戦略が考えられる．

ミクログリアと炎症反応●

孤発性 PD 患者剖検脳や家族性 PD 患者剖検脳，さらに MPTP 誘導性 PD モデル動物脳の黒質線条体部において共通にみられる病理変化として，ミクログリアの活性化と集積がある．ミクログリアは活性化すると HLA-DR や iNOS や COX-2 を発現し，インターロイキン(IL)-1βや IL-6 などの炎症性サイトカインを含む種々のサイトカインを産生し，炎症反応の特徴の多くを示す．また，活性化したミクログリアは炎症性サイトカイン以外に，活性酸素や NO，プロテアーゼ類などの神経傷害性因子も産生する．とくに活性酸素や NO などのフリーラジカルは PD における神経変性の進行機序に関与するため，ミクログリ

アの活性化や脳内炎症反応はPDの発症や進行に密接に関わっている[17]．MPTP曝露16年後の死後，脳においても活性化ミクログリアが存在し，ミクログリアの活性化を伴う長期間にわたる継続的な炎症状態がPDの病態の進行において重要な意味をもつ可能性を示唆している．GWASでHLA-DR抗原の領域が同定されたことも興味深い[11]．

おわりに

PDのメカニズムの解明にあたっては，メンデル遺伝型PDの原因遺伝子の研究成果が大きく貢献してきた．今後は未知のメンデル遺伝型遺伝子の同定のみならず，孤発性PDにおいて大規模なGWAS，rare variant解析から，新規の感受性遺伝子が同定され，新しい機序，創薬の手がかりがみつかる可能性がある．次世代シークエンサーによるエキソームリシークエンスも開始され，今後はパーソナルゲノム解析が医学研究に応用されよう．

また，プリオン仮説は異常蛋白凝集を特徴とする神経変性疾患に共通した病態機序である可能性がある．同時に，異常蛋白の細胞間伝播は神経変性疾患に共通の治療ターゲットとなる可能性を秘めており，今後に期待する．

文　献

1) Farrer MJ：Genetics of Parkinson disease：paradigm shifts and future prospects. Nat Rev Genet **7**：306, 2006
2) Fujiwara H et al：alpha-Synuclein is phosphorylated in synucleinopathy lesions. Nat Cell Biol **4**：160, 2002
3) Uversky VN：Neuropathology, biochemistry, and biophisics of alpha-synuclein aggregation. J Neurohem **103**：17, 2007
4) Cooper AA et al：Alpha-synuclein blocks ER-Golgi traffic and Rab1 rescues neuron loss in Parkinson's models. Science **313**：324, 2006
5) McNaught KS et al：Proteasomal dysfunction in sporadic Parkinson's disease. Neurology **66**[Suppl 4]：S37, 2006
6) Martinez-Vicente M, Cuervo AM：Autophagy and neurodegeneration：when the cleaning crew goes on strike. Lancet Neurol **6**：352, 2007
7) Gitler AD et al：Alpha-synuclein is part of a diverse and highly conserved interaction network that includes PARK9 and manganese toxicity. Nat Genet **41**：308, 2009
8) Schapira AH：Mitochondria in the aetiology and pathogenesis of Parkinson's disease. Lancet Neurol **7**：97, 2008
9) Narendra DP et al：PINK1 is selectively stabilized on impaired mitochondria to activate Parkin. PLoS Biol **28**：e1000298, 2010
10) Satake W et al：Genome-wide association study identifies common variants at four loci as genetic risk factors for Parkinson's disease. Nat Genet **41**：1303, 2009
11) Hamza TH et al：Common genetic variation in the HLA region is associated with late-onset sporadic Parkinson's disease. Nat Genet **42**：781, 2010
12) Mitsui J et al：Mutations for Gaucher disease confer a high susceptibility to Parkinson disease. Arch Neurol **66**：571, 2009
13) Sidransky E et al：Multicenter analysis of glucocerebrosidase mutations in Parkinson's disease. N Engl J Med **361**：1651, 2009
14) Li JY et al：Lewy bodies in grafted neurons in subjects with Parkinson's disease suggest host-to-graft disease propagation. Nat Med **14**：501, 2008
15) Hansen C et al：α-Synuclein propagates from mouse brain to grafted dopaminergic neurons and seeds aggregation in cultured human cells. J Clin Invest **121**：715, 2011
16) Olanow CW, Prusiner SB：Is Parkinson's disease a prion disorder? Proc Natl Acad Sci U S A **106**：12571, 2009
17) Sawada M et al：Effects of aging on neuroprotective and neurotoxic properties of microglia in neurodegenerative diseases. Neurodegener Dis **5**：254, 2008

Neurobiology of Disease 41 (2011) 111–118

Contents lists available at ScienceDirect

Neurobiology of Disease

journal homepage: www.elsevier.com/locate/ynbdi

Mitochondrial membrane potential decrease caused by loss of PINK1 is not due to proton leak, but to respiratory chain defects

Taku Amo [a,1], Shigeto Sato [b], Shinji Saiki [b], Alexander M. Wolf [a], Masaaki Toyomizu [c], Clement A. Gautier [d], Jie Shen [d], Shigeo Ohta [a], Nobutaka Hattori [b,*]

[a] Department of Biochemistry and Cell Biology, Institute of Development and Aging Sciences, Graduate School of Medicine, Nippon Medical School, 1-396 Kosugi-cho, Nakahara-ku, Kawasaki 211-8533, Japan
[b] Department of Neurology, Juntendo University School of Medicine, 2-1-1 Hongo, Bunkyo-ku, Tokyo 113-8421, Japan
[c] Animal Nutrition, Life Sciences, Graduate School of Agricultural Science, Tohoku University, 1-1 Tsutsumidori-Amamiyamachi, Aoba-ku, Sendai 981-8555, Japan
[d] Center for Neurologic Diseases, Brigham and Women's Hospital, Program in Neuroscience, Harvard Medical School, Boston, MA 02115, USA

ARTICLE INFO

Article history:
Received 29 June 2010
Revised 17 August 2010
Accepted 25 August 2010
Available online 15 September 2010

Keywords:
Parkinson's disease
Mitochondria
PINK1
Parkin
Membrane potential
Oxidative phosphorylation
Modular kinetic analysis
Proton leak
Reactive oxygen species

ABSTRACT

Mutations in *PTEN-induced putative kinase 1* (*PINK1*) cause a recessive form of Parkinson's disease (PD). PINK1 is associated with mitochondrial quality control and its partial knock-down induces mitochondrial dysfunction including decreased membrane potential and increased vulnerability against mitochondrial toxins, but the exact function of PINK1 in mitochondria has not been investigated using cells with null expression of PINK1. Here, we show that loss of PINK1 caused mitochondrial dysfunction. In PINK1-deficient ($PINK1^{-/-}$) mouse embryonic fibroblasts (MEFs), mitochondrial membrane potential and cellular ATP levels were decreased compared with those in littermate wild-type MEFs. However, mitochondrial proton leak, which reduces membrane potential in the absence of ATP synthesis, was not altered by loss of PINK1. Instead, activity of the respiratory chain, which produces the membrane potential by oxidizing substrates using oxygen, declined. H_2O_2 production rate by $PINK1^{-/-}$ mitochondria was lower than $PINK1^{+/+}$ mitochondria as a consequence of decreased oxygen consumption rate, while the proportion (H_2O_2 production rate per oxygen consumption rate) was higher. These results suggest that mitochondrial dysfunctions in PD pathogenesis are caused not by proton leak, but by respiratory chain defects.

Introduction

Parkinson's disease (PD) is a neurodegenerative disease characterized by loss of dopaminergic neurons in the substantia nigra. Mitochondrial dysfunction has been proposed as a major factor in the pathogenesis of sporadic and familial PD (Abou-Sleiman et al., 2006). In particular, the identification of mutations in *PTEN-induced putative kinase 1* (*PINK1*) has strongly implicated mitochondrial dysfunction owing to its loss of function in the pathogenesis of PD (Valente et al., 2004). PINK1 contains an N-terminal mitochondrial targeting sequence (MTS) and a serine/threonine kinase domain (Valente et al., 2004). PINK1 kinase activity is crucial for mitochondrial maintenance via TRAP phosphorylation (Pridgeon et al., 2007). Loss of PINK1 function induces increased vulnerability to various stresses (Exner et al., 2007; Haque et al., 2008; Pridgeon et al., 2007; Wood-Kaczmar et al., 2008). However, silencing of PINK1 has only been partial and only one study has been performed to assess mitochondrial functions in steady and artificial states with complete ablation of PINK1 expression (Gautier et al., 2008).

Several studies have shown that PINK1 acts upstream of parkin in the same genetic pathway (Clark et al., 2006; Park et al., 2006) and co-overexpressed PINK1 and parkin both co-localized to mitochondria (Kim et al., 2008). Overexpression of PINK1 promotes mitochondrial fission (Yang et al., 2008). Fission followed by selective fusion segregates dysfunctional mitochondria and permits their removal by autophagy (Twig et al., 2008). PINK1 loss-of-function decreases mitochondrial membrane potential (Chu, 2010) and the PINK1–parkin pathway is associated with mitochondrial elimination in cultured cells treated with the mitochondrial uncoupler carbonyl cyanide *m*-chlorophenylhydrazone (CCCP), which causes mitochondrial depolarization (Geisler et al., 2010; Kawajiri et al., 2010; Matsuda et al., 2010; Narendra et al., 2008, 2010; Vives-Bauza et al., 2010). However, the exact mechanism underlying the mitochondrial depolarization induced by PINK1 defects leading to mitochondrial autophagy has not been examined in detail.

Abbreviations: $\Delta\psi$, mitochondrial membrane potential; FCCP, carbonyl cyanide *p*-trifluoromethoxyphenylhydrazone; MEFs, mouse embryonic fibroblasts; PD, Parkinson's disease; PINK1, PTEN-induced putative kinase 1; ROS, reactive oxygen species; TMRM, tetramethylrhodamine methyl ester; TPMP, triphenylmethylphosphonium.

* Corresponding author. Fax: +81 3 5800 0547.
E-mail address: nhattori@juntendo.ac.jp (N. Hattori).
[1] Present address: Department of Applied Chemistry, National Defense Academy, 1-10-20 Hashirimizu, Yokosuka 239-8686, Japan.

Available online on ScienceDirect (www.sciencedirect.com).

0969-9961/$ – see front matter © 2010 Elsevier Inc. All rights reserved.
doi:10.1016/j.nbd.2010.08.027

Here, we describe a detailed characterization of mitochondria in PINK1-deficient cells. We show that PINK1 deficiency causes a decrease in mitochondrial membrane potential, which is not due to proton leak, but to respiratory chain defects.

Materials and methods

PINK1 knock-out mouse embryonic fibroblasts (MEFs)

PINK1 knock-out MEFs were prepared and cultured as described previously (Matsuda et al., 2010). Mouse embryonic fibroblasts (MEFs) were derived from E12.5 embryos containing littermate 4 mice of each genotype. Embryos were mechanically dispersed by repeated passage through a P1000 pipette tip and plated with MEF media containing DME, 10% FCS, 1× nonessential amino acids, 1 mM L-glutamine, penicillin/streptomycin (invitrogen). The ψ2 cell line, an ecotropic retrovirus packaging cell line, was maintained in Dulbecco's modified Eagle medium (DMEM, Sigma) with 5% fetal bovine serum and 50 μg/ml kanamicin. Transfection of the ψ2 cells with pMESVTS plasmids containing an SV40 large T antigen was performed by lipofection method according to the manual provided by the manufacturer (GIBCO BRL). Five micrograms of the plasmids was used for each transfection. Transfectants were selected by G418 at the concentration of 0.5 mg/ml, and 10 clonal cell lines were established. The highest titer of 5×10^4 cfu/ml was obtained for the conditioned medium of a cell line designated ψ2SVTS1. 10^6 MEFs were plated onto a 10-cm culture dish and kept at 33 °C for 48 hours. Then medium was replaced with 2 ml supplemented with polybrene-supplemented medium conditioned by the ψ2SVTS1 cells at confluency for 3 days. Infection was continued for 3 hours, and the medium was replaced with a fresh one. The infected MEFs were cultured at 33 °C until immortalized cells were obtained.

We confirmed that the differences we detected in this study were due to the PINK1 deficiency, not to artificial effects by immortalization, by measuring cellular respiration rates of not immortalized MEFs from other littermates (Supplemental figure). The respiration rates of not immortalized MEFs were slightly slower than those of immortalized MEFs, but the differences between $PINK1^{+/+}$ and $^{-/-}$ MEFs were consistent (Fig. 2A).

Cell growth

Cells were seeded in 12-well plates at density of $3\sim6\times10^3$ cells/well and incubated in DMEM high glucose medium (4.5 g/l glucose and 1 mM sodium pyruvate) supplemented with 10% fetal bovine serum. After a day, the medium was replaced with DMEM glucose-free medium supplemented with 1 g/l galactose, 1 mM sodium pyruvate and 10% fetal bovine serum (DMEM galactose medium) at 37 °C in an incubator with a humidified atmosphere of 5% CO_2. Cells were trypsinized and live cells were assessed by trypan blue dye exclusion.

Mitochondrial morphological changes

Cells were seeded in 6-well plates at 2.0×10^5/well and incubated in DMEM high glucose medium (4.5 g/l glucose and 1 mM sodium pyruvate) supplemented with 10% fetal bovine serum and 1% penicillin/streptomycin. After a day, the medium was replaced with DMEM glucose-free medium supplemented with 1 g/l galactose, 1 mM sodium pyruvate and 10% fetal bovine serum (DMEM galactose medium) at 37 °C in an incubator with a humidified atmosphere of 5% CO_2. 24 hours later, cells were fixed and immunostained with anti-Tom20 antibody to visualize mitochondria according to a protocol as previously described (Kawajiri et al., 2010). All images were obtained using an Axioplan 2 imaging microscope (Carl Zeiss, Oberkochen, Germany).

Cellular ATP levels

Intracellular ATP levels were determined by a cellular ATP assay kit (TOYO B-Net, Tokyo, Japan) according to the manufacturer's instructions using a Lumat LB9507 luminometer (Berthold Technology, Bad Wildbad, Germany).

Membrane potential

Fluorescence images were recorded using a multi-dimensional imaging workstation (AS MDW, Leica Microsystems, Wetzlar, Germany) with a climate chamber maintained at 37 °C. Fluorescence was quantified with a CCD camera (CoolSnap HQ, Roper Scientific, Princeton, NJ) using a 20× objective. Cells were stained for 1 hour with a non-quenching concentration (20 nM) of tetramethylrhodamine methyl ester (TMRM) in a 96-well plate. The cell-permeable cationic dye TMRM accumulates in mitochondria according to the Nernst equation. Nuclei were stained with 250 nM Hoechst 34580. Mitochondrial TMRM fluorescence was integrated in a 40-μm diameter circular area around the nucleus, and the minimum fluorescence in this area was subtracted as background fluorescence.

Cell respiration

Cell respiration was measured at 37 °C using the Oxygen Meter Model 781 and the Mitocell MT200 closed respiratory chamber (Strathkelvin Instruments, North Lanarkshire, United Kingdom). Cells were cultured in DMEM with 4.5 g/l of glucose supplemented with 10% FBS. Cells were then trypsinized and resuspended in Leibovitz's L-15 medium (Invitrogen) at density of 8.0×10^6 cells/ml. The oxygen respiration rate was measured under each of the following three conditions: basal rate (no additions); State 4 (no ATP synthesis) [after addition of 1 μg/ml oligomycin (Sigma)], uncoupled [after addition of 3 μM FCCP (carbonyl cyanide *p*-trifluoromethoxyphenylhydrazone; Sigma)] using Strathkelvin 949 Oxygen System. After sequential measurements, the endogenous respiration rate was determined by adding 1 μM rotenone + 2 μM myxothiazol.

Mitochondrial respiration and membrane potential

Mitochondria were prepared from cultured MEFs as previously described (Amo and Brand, 2007). Mitochondrial oxygen consumption with 5 mM succinate as a respiratory substrate was measured at 37 °C using a Clark electrode (Rank Brothers, Cambridge, United Kingdom) calibrated with air-saturated respiration buffer comprising 0.115 M KCl, 10 mM KH_2PO_4, 3 mM HEPES (pH 7.2), 2 mM $MgCl_2$, 1 mM EGTA and 0.3% (w/v) defatted BSA, assumed to contain 406 nmol atomic oxygen/ml (Reynafarje et al., 1985). Mitochondrial membrane potential ($\Delta\psi$) was measured simultaneously with respiratory activity using an electrode sensitive to the lipophilic cation $TPMP^+$ (triphenylmethylphosphonium) (Brand, 1995). Mitochondria were incubated at 0.5 mg/ml in the presence of 80 ng/ml nigericin (to collapse the pH gradient so that the proton motive force was expressed exclusively as $\Delta\psi$) and 2 μM rotenone (to inhibit complex I). The $TPMP^+$-sensitive electrode was calibrated with sequential additions of $TPMP^+$ up to 2 μM, then 5 mM succinate was added to initiate respiration. Experiments were terminated with 2 μM FCCP, allowing correction for any small baseline drift. $\Delta\psi$ was calculated from the distribution of $TPMP^+$ across the mitochondrial inner membrane using a binding correction factor of 0.35 mg protein/μl. Respiratory rates with 4 mM pyruvate + 1 mM malate as a substrate in State 3 (with 0.25 mM ADP) and State 4 (with 1 μg/ml oligomycin) were determined using the Oxygen Meter Model 781 and the Mitocell MT200 closed respiratory chamber (Strathkelvin Instruments).

Modular kinetic analysis

To investigate differences in oxidative phosphorylation caused by PINK1 knock-out, we applied a systems approach, namely modular kinetic analysis (Amo and Brand, 2007; Brand, 1990). This analyzes the kinetics of the whole of oxidative phosphorylation divided into three modules connected by their common substrate or product, $\Delta\psi$. The modules are (i) the reactions that produce $\Delta\psi$, consisting of the substrate translocases, dehydrogenases and other enzymes and the components of the respiratory chain, called 'substrate oxidation'; (ii) the reactions that consume $\Delta\psi$ and synthesize, export and dephosphorylate ATP, consisting of ATP synthase, the phosphate and adenine nucleotide translocases and any ATPases that may be present, called the 'phosphorylating system'; and (iii) the reactions that consume $\Delta\psi$ without ATP synthesis, called the 'proton leak' (Brand, 1990). The analysis reports changes anywhere within oxidative phosphorylation that are functionally important but is unresponsive to changes that have no functional consequences. Comparison of the kinetic responses of each of the three modules to $\Delta\psi$ obtained using mitochondria isolated from PINK1$^{+/+}$ and PINK1$^{-/-}$ MEFs would reveal any effects of PINK1 on the kinetics of oxidative phosphorylation. Oxygen consumption and $\Delta\psi$ were measured simultaneously using mitochondria incubated with 80 ng/ml nigericin and 4 μM rotenone. Respiration was initiated by 5 mM succinate. The kinetic behavior of a '$\Delta\psi$-producer' can be established by specific modulation of a $\Delta\psi$-consumer and the kinetics of a consumer can be established by specific modulation of a $\Delta\psi$-producer (Brand, 1998). To measure the kinetic response of proton leak to $\Delta\psi$, the State 4 (non-phosphorylating) respiration of mitochondria in the presence of oligomycin (0.8 μg/ml; to prevent any residual ATP synthesis), which was used solely to drive the proton leak, was titrated with malonate (up to 8 mM). In a similar way, State 4 respiration was titrated by FCCP (up to 1 μM) for measurement of the kinetic response of substrate oxidation to $\Delta\psi$. State 3 (maximal rate of ATP synthesis) was obtained by addition of excess ADP (1 mM). Titration of State 3 respiration with malonate (up to 1.1 mM) allowed measurement of the kinetics of the $\Delta\psi$-consumers (the sum of the phosphorylating system and proton leak). The coupling efficiencies of oxidative phosphorylation were calculated from the kinetic curves as the percentage of mitochondrial respiration rate at a given $\Delta\psi$ that was used for ATP synthesis and was therefore inhibited by oligomycin. Note that any slip reactions will appear as proton leak in this analysis (Brand et al., 1994).

Mitochondrial ROS production

Mitochondrial ROS production rate was assessed by measurement of H_2O_2 generation rate, determined fluorometrically by measurement of oxidation of Amplex Red to fluorescent resorufin coupled to the enzymatic reduction of H_2O_2 by horseradish peroxidase using a spectrofluorometer RF-5300PC (Shimadzu, Kyoto, Japan). The H_2O_2 generation rate was measured in non-phosphorylating conditions (=State 4) using either pyruvate/malate or succinate as respiratory substrates. Mitochondria were incubated at 0.1 mg/ml in respiration buffer. All incubations also contained 5 μM Amplex Red, 2 U/ml horseradish peroxidase and 8 U/ml superoxide dismutase. The reaction was initiated by addition of 5 mM succinate or 4 mM pyruvate + 1 mM malonate and the increase in fluorescence was followed at excitation and emission wavelengths of 560 and 590 nm, respectively. Appropriate correction for background signals and standard curves generated using known amounts of H_2O_2 were used to calculate the rate of H_2O_2 production in nmol/min/mg mitochondrial protein. The percentage free radical leak, which is a measure of the number of electrons that produce superoxide (and subsequently H_2O_2) compared with the total number of electrons which pass thorough the respiratory chain, was calculated as the rate of H_2O_2 production divided by the rate of O_2 consumption (Barja et al., 1994).

Statistics

Values are presented as means ± SEM except Fig. 2D, in which error bars indicate SD. The significance of differences between means was assessed by the unpaired Student's *t*-test using Microsoft Excel; *P* values < 0.05 were taken to be significant.

Results

Cell growth and mitochondrial morphology

In general, cultured cells gain their energy mostly from glycolysis. Therefore, cells deficient in respiratory function can grow in normal medium, although possibly at a slower rate, relying predominantly on glycolysis (Hofhaus et al., 1996). Actually, ρ^0 cells, which lack mitochondrial DNA completely, can grow producing energy exclusively through glycolysis (King and Attardi, 1989). On the other hand, galactose metabolism via glycolysis is much slower than glucose metabolism (Reitzer et al., 1979). Therefore, cells in galactose medium are forced to oxidize pyruvate through the mitochondrial respiratory chain for energy required for growth. Consequently, cells with defects in their mitochondrial respiratory chains show growth impairments in galactose medium. To evaluate this phenomenon is also observed in our cells, we examined growth retardation by addition of mitochondrial complex I inhibitor, rotenone (Fig. 1A). In glucose medium, 10 nM rotenone had only a slight effect on the growth of PINK1$^{+/+}$ MEFs and slower growth was observed even in the presence of 100 nM rotenone. However, in the galactose medium, 10 nM rotenone significantly inhibited the growth of PINK1$^{+/+}$ MEFs and 100 nM roteone completely arrested the growth. Therefore, we could confirm that the growth impairment of our cells in the galactose medium was due to mitochondrial respiratory chain defects.

PINK1 acts upstream of parkin, regulating mitochondrial integrity and function; therefore, loss of PINK1 is considered to affect mitochondrial functions. To assess the mitochondrial functions of PINK1$^{-/-}$ MEFs, growth capability in a medium in which galactose replaced glucose was examined. As shown in Fig. 1B, PINK1$^{-/-}$ MEFs appeared to show clear growth impairments in the galactose medium, whereas PINK1$^{+/+}$ MEFs grew slightly slower than in the glucose medium.

No differences of mitochondrial morphology between PINK1$^{+/+}$ and $^{-/-}$ MEFs in the glucose medium were detected (Fig. 1C), consistent with the previous report (Matsuda et al., 2010). However, in the galactose medium, mitochondria of the PINK1$^{-/-}$ MEFs were more fragmented compared to the PINK$^{+/+}$ MEFs (Fig. 1C). This is consistent with previous reports, which found mitochondrial morphological changes were more pronounced when PINK1 knock-down HeLa cells were grown in low-glucose medium (Exner et al., 2007) and human PINK1 homozygous mutant fibroblast in galactose medium (Grünewald et al., 2009). In these cells, mitochondrial morphological changes were associated with the mitochondrial functional impairment.

Assessments of mitochondrial functions at the cellular level

Because PINK1$^{-/-}$ MEFs showed severe growth impairments in the galactose medium, the mitochondrial functions of these cells were assessed at the cellular level. First, cellular respiration rates were measured (Fig. 2A). The basal respiration rate was significantly reduced in PINK1$^{-/-}$ cells compared with that in PINK1$^{+/+}$ cells (11.13 ± 0.71 versus 14.36 ± 1.01 nmol O/min/10^6 cells; $p<0.05$; $n=5$ independent experiments), consistent with previous reports using partial knock-down of PINK1 expression (Gandhi et al., 2009; Liu et al., 2009). Oligomycin inhibits ATP synthase, resulting in non-phosphorylating respiration. FCCP uncouples oxidative phosphorylation, leading to maximum respiration rates. In both conditions, the

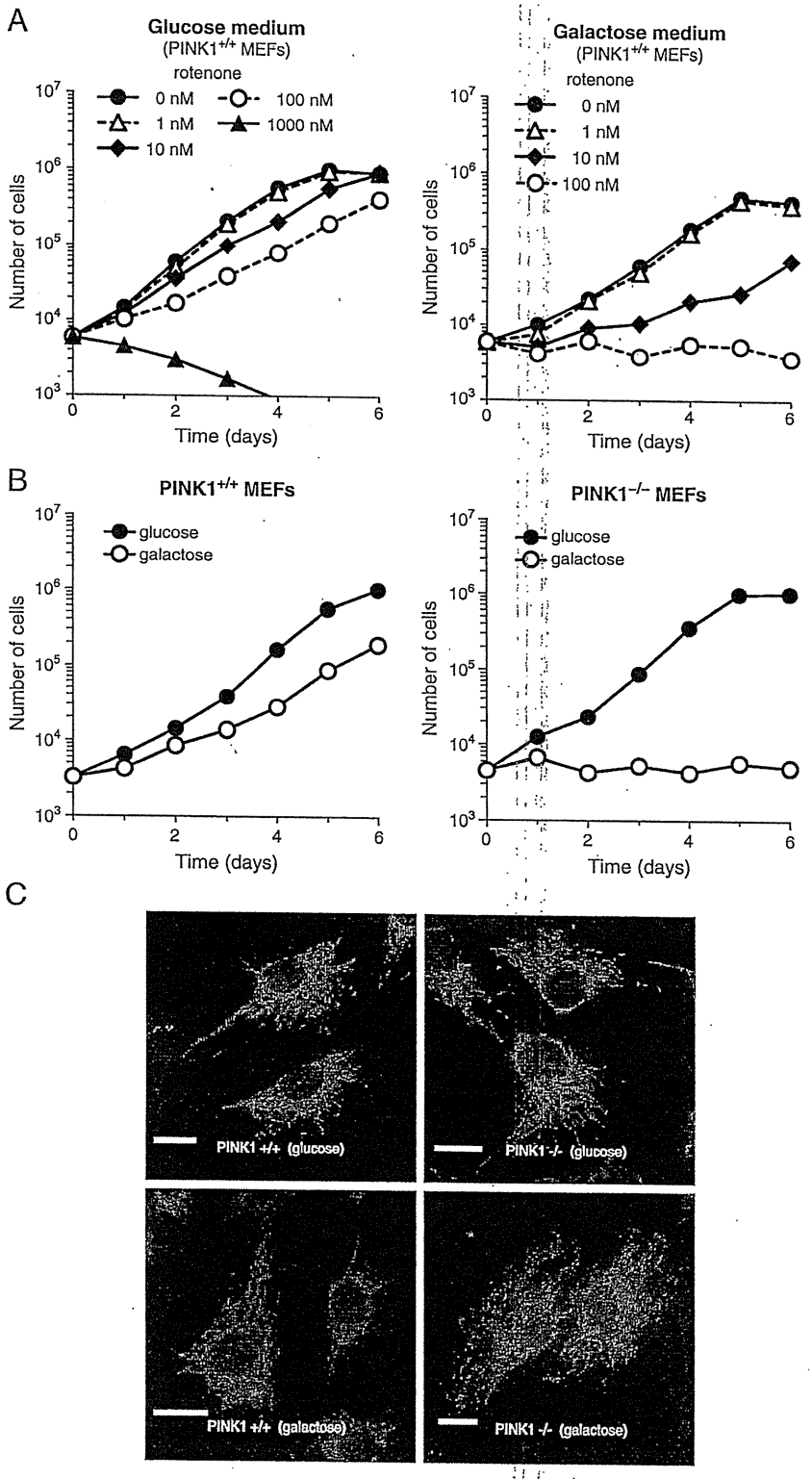

Fig. 1. (A) Growth retardation of PINK1$^{+/+}$ MEFs by mitochondrial complex I inhibitor, rotenone in glucose or galactose medium. Closed circles with solid line, 0 nM rotenone; open triangles with dashed line, 1 nM rotenone; closed diamonds with solid line, 10 nM rotenone; open circles with dashed line, 100 nM rotenone; closed triangles with solid line, 1000 nM rotenone. Cells grown in 12-well plates were trypsinized and live cells were assessed by trypan blue dye exclusion. (B) Growth curves of PINK1$^{+/+}$ and $^{-/-}$ MEFs. Closed symbols (*glucose*), growth curve for cells grown in DMEM containing 4.5 g/l glucose and 1 mM sodium pyruvate; open symbols (*galactose*), growth curve for cells grown in DMEM lacking glucose and containing instead 1.0 g/l galactose and 1 mM sodium pyruvate. Cells grown in 12-well plates were trypsinized and live cells were assessed by trypan blue dye exclusion. (C) Mitochondrial morphology of PINK1$^{+/+}$ and $^{-/-}$ MEFs. After incubating cells with the glucose or galactose medium for 24 hours, cells were fixed and immunostained with anti-Tom20 antibody to visualize mitochondria. Scale bar, 20 μm.

PINK1$^{-/-}$ cells respired significantly slower than the PINK1$^{+/+}$ cells (1.76 ± 0.13 versus 2.95 ± 0.27 ($p<0.01$; $n=5$ independent experiments) and 16.44 ± 1.80 versus 23.50 ± 1.18 nmol O/min/10^6 cells ($p<0.05$; $n=5$ independent experiments), respectively).

The main function of mitochondria is ATP synthesis via oxidative phosphorylation. ATP levels under basal conditions were significantly reduced in PINK1$^{-/-}$ MEFs (Fig. 2B), as reported previously for dissociated PINK1$^{-/-}$ mouse neurons (Gispert et al., 2009) and PINK1

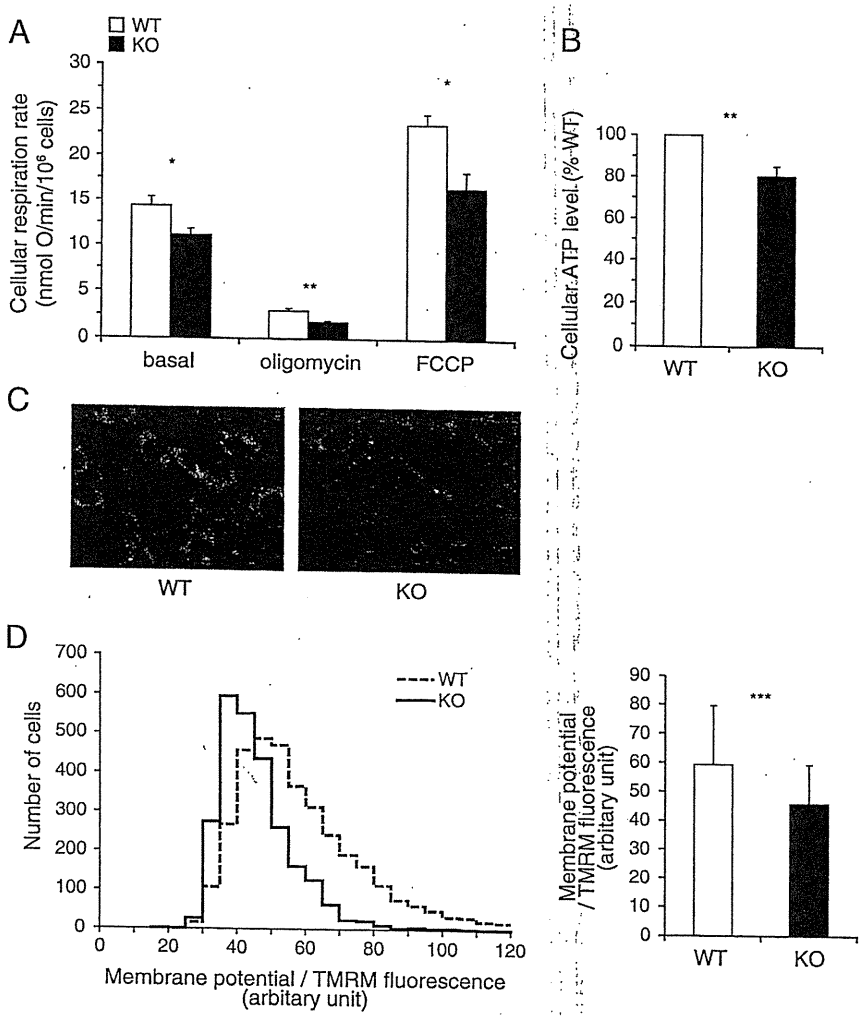

Fig. 2. Mitochondrial functions assessed at the cellular level. Open bars, PINK1$^{+/+}$ MEFs; closed bars, PINK1$^{-/-}$ MEFs. (A) Cell respiration rate of PINK1$^{+/+}$ and $^{-/-}$ MEFs. The oxygen respiration rate was measured at density of 8.0×10^6 cells/ml under each of the following three conditions: basal rate (no additions); State 4 (no ATP synthesis) [after addition of 1 μg/ml oligomycin], uncoupled [after addition of 3 μM FCCP]. After sequential measurements, the endogenous respiration rate was determined by adding 1 μM rotenone + 2 μM myxothiazol. Error bars indicate SEM ($n=5$ independent experiments). (B) Cellular ATP levels. Data were normalized based on cell numbers and expressed as the percentage of the level in PINK1$^{+/+}$ cells. Error bars indicate SEM ($n=4$ independent experiments). (C) Live cell images of PINK1$^{+/+}$ and $^{-/-}$ MEFs with TMRM fluorescence. (D) Mitochondrial membrane potential evaluated by live cell imaging of TMRM fluorescence. *Left panel*, the distribution of TMRM fluorescence from 3537 PIINK1$^{+/+}$ and 2566 PINK1$^{-/-}$ cells from 12 wells per cell type; *right panel*, the average value of TMRM fluorescence per cell. Error bars indicate SD. $^*P<0.05$; $^{**}P<0.01$; $^{***}P<0.001$.

siRNA knock-down PC12 cells (Liu et al., 2009). Mitochondrial membrane potential was also measured by live cell imaging of TMRM fluorescence. Typical images were shown in Fig. 2C. The histogram shows the distribution of TMRM fluorescence from 3537 PINK1$^{+/+}$ cells and 2566 PINK1$^{-/-}$ cells from 12 wells per cell type and the bar graph indicates the mean ± SD of TMRM fluorescence per cell (Fig. 2D). According to the Nernst equation, the ratio of TMRM fluorescence would translate into, on average, 6.88 mV lower mitochondrial membrane potential in the PINK1$^{-/-}$ cells if the plasma membrane potentials were not different between PINK1$^{+/+}$ and $^{-/-}$ cells. Mitochondrial membrane potential decrease was also showed previously in PINK1 knock-down HeLa cells (Exner et al., 2007) and in stable PINK1 knock-down neuroblastoma cell lines (Sandebring et al., 2009).

Assessments of mitochondrial functions using isolated mitochondria

To further analyze mitochondrial functions, we measured the kinetics of oxidative phosphorylation using isolated mitochondria from PINK1$^{+/+}$ and $^{-/-}$ MEFs. Fig. 3 shows the kinetics of the three modules of oxidative phosphorylation using succinate as a respiratory substrate (complex II-linked respiration). Fig. 3A shows the kinetic response of substrate oxidation to its product, $\Delta\psi$. The substrate oxidation kinetic curve for PINK1$^{-/-}$ cells was clearly shifted lower compared with that for PINK1$^{+/+}$ cells, indicating that the loss of PINK1 caused mitochondrial respiratory chain defects. Fig. 3B shows the kinetic response of proton leak to its driving force, $\Delta\psi$, and Fig. 3C shows the kinetic response of the ATP phosphorylating pathway to its driving force, $\Delta\psi$. Both kinetic curves for PINK1$^{+/+}$ and $^{-/-}$ MEFs (open and closed symbols, respectively) were overlapping, implying that there were no significant differences in those modules.

We also independently measured the mitochondrial oxygen consumption rate using pyruvate/malate as a respiratory substrate instead of succinate to check complex I. Modular kinetic analysis using pyruvate/malate is technically difficult for the following reasons: (1) the oxygen consumption rate with pyruvate/malate is much slower than succinate respiration; and (2) there are no competitive inhibitors of complex I-linked respiration, such as malonate for succinate respiration. As shown in Fig. 4A, the respiration rates in State 3 and 4 with pyruvate/malate of isolated mitochondria from PINK1$^{-/-}$ cells (closed symbols) were significantly slower than those of PINK1$^{+/+}$ cells (open symbols), as in the case of succinate respiration (Fig. 4B; data derived from the kinetic curves in Fig. 3).

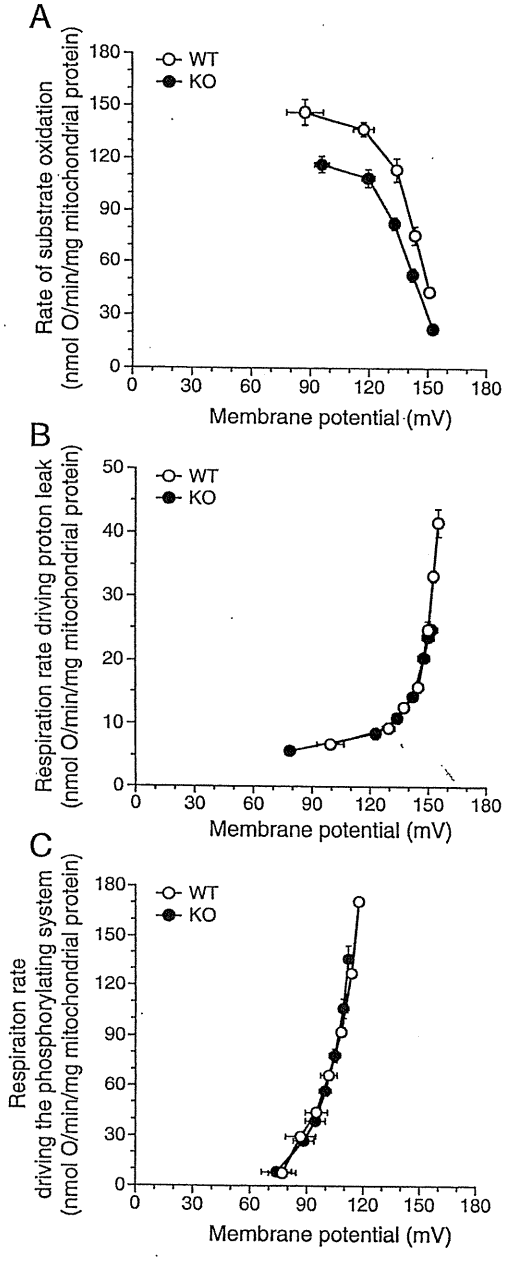

Fig. 3. Modular kinetic analysis of oxidative phosphorylation in mitochondria isolated from PINK1$^{+/+}$ and $^{-/-}$ MEFs. Modular kinetic analysis of the kinetic responses to membrane potential, $\Delta\psi$, of respiration driving (A) substrate oxidation ($\Delta\psi$ titrated with uncoupler, FCCP, starting in State 4), (B) proton leak ($\Delta\psi$ titrated with malonate, starting in State 4) and (C) the phosphorylating system, calculated by subtracting respiration driving proton leak from respiration driving the $\Delta\psi$-consumers ($\Delta\psi$ titrated with malonate starting in State 3; not shown) at each $\Delta\psi$. Open symbols, PINK1$^{+/+}$ MEFs; closed symbols, PINK1$^{-/-}$ MEFs. Error bars indicate SEM ($n=4$ independent mitochondrial preparations).

Mitochondrial ROS production

Mitochondrial ROS production rate was assessed by measurement of the H_2O_2 generation rate. Mechanisms of mitochondrial ROS production were well described elsewhere (Fig. 1 of Lambert et al., 2010). Pyruvate and malate generate NADH, which induced forward electron transport and generate ROS mainly from complex I and III. For pyruvate/malate respiration, the basal H_2O_2 generation rate (measured in the absence of respiratory chain inhibitors) was not different between PINK1$^{+/+}$ and $^{-/-}$ mitochondria (Fig. 4C). The addition of antimycin A and further addition of rotenone, which inhibited forward electron transport at complex III and I, respectively, enhanced H_2O_2 generation. During succinate respiration in the absence of respiratory chain inhibitors, ROS are generated mainly from the quinine binding site of complex I due to reverse electron flow from coenzyme Q to complex I. For succinate respiration, H_2O_2 generation rate in the absence of reparatory chain inhibitors was higher in PINK1$^{+/+}$ mitochondria than in PINK1$^{-/-}$ mitochondria, but the difference was not significant (Fig. 4D). The addition of rotenone, which blocks reverse electron flow from coenzyme Q to complex I, attenuated H_2O_2 generation.

Figs. 4 C and D show a tendency for PINK1$^{+/+}$ mitochondria to generate more ROS than PINK1$^{-/-}$ mitochondria. However, their respiration rates were remarkably different (Figs. 4A and B). Therefore, we calculated the percentage free radical leak, which is the fraction of molecules of O_2 consumed that give rise to H_2O_2 release by mitochondria (free radical leak) during either pyruvate/malate or succinate State 4 respiration (Figs. 4E and F). For pyruvate/malate respiration, mitochondria isolated from PINK1$^{-/-}$ cells had higher proportion of H_2O_2 generation than PINK1$^{+/+}$ mitochondria. During succinate respiration without respiratory inhibitors, PINK1$^{-/-}$ mitochondria had also higher proportion of free radical leak mainly from complex I due to reverse electron flow from coenzyme Q to complex I. Because the differences disappeared with addition of rotenone, which inhibit reverse electron flow, ROS generation enhanced by loss of PINK1 was mostly from complex I.

Discussion

We produced an *in vitro* model of Parkinson's disease, immortalized PINK1$^{-/-}$ MEFs. Previously, impairment of mitochondrial respiration was observed in the brains of PINK1$^{-/-}$ mice (Gautier et al., 2008). PINK1$^{-/-}$ MEFs clearly showed a phenotype of mitochondrial dysfunctions, which is consistent with PD pathogenesis. This phenotype was apparent in a cell growth experiment using medium containing galactose instead of glucose (Fig. 1B). Mitochondrial fragmentation was observed when PINK1$^{-/-}$ MEFs grew in the galactose medium (Fig. 1C), which was consistent with previous reports (Exner et al., 2007; Grünewald et al., 2009). Our results have unveiled that the PINK1$^{-/-}$ MEF line could be a potential PD model, presenting growth retardation due to decreased mitochondrial respiration activity. Thus, the PINK1$^{-/-}$ MEFs are a useful tool for evaluating the role of PINK1 in mitochondrial dysfunction and relevant to PD.

In PINK1$^{-/-}$ MEFs, mitochondrial membrane potential was decreased compared with that in littermate wild-type MEFs (Figs. 2C and D), as reported previously for PINK1 knock-down HeLa cells (Exner et al., 2007) and stable PINK1 knock-down neuroblastoma cell lines (Sandebring et al., 2009). This is a key event during elimination of mitochondria. Mitochondrial fission followed by selective fusion segregates damaged mitochondria, which decreases their membrane potential, and permits their removal by autophagy (Twig et al., 2008). The PINK1–parkin pathway is thought to have a crucial role in this mitochondrial elimination mechanism (Geisler et al., 2010; Kawajiri et al., 2010; Matsuda et al., 2010; Narendra et al., 2008, 2010; Vives-Bauza et al., 2010). To clarify what caused the decrease in mitochondrial membrane potential, we performed a modular kinetic analysis using isolated mitochondria (Fig. 3). This analyzes the kinetics of the whole of oxidative phosphorylation divided into three modules connected by their common substrate or product, mitochondrial membrane potential ($\Delta\psi$). The modules are include one $\Delta\psi$-producer (substrate oxidation) and two $\Delta\psi$-consumers (phosphorylating system and proton leak) (Brand, 1990). To decrease $\Delta\psi$, the $\Delta\psi$-producer should be down-regulated and/or $\Delta\psi$-consumers should be up-regulated. As cellular ATP levels were decreased compared with those in littermate wild-type MEFs (Fig. 2B), it is unlikely that the phosphorylating system is up-regulated. Indeed, the kinetics of the phosphorylation module were not altered (Fig. 3C). The other $\Delta\psi$-consumer, proton leak,

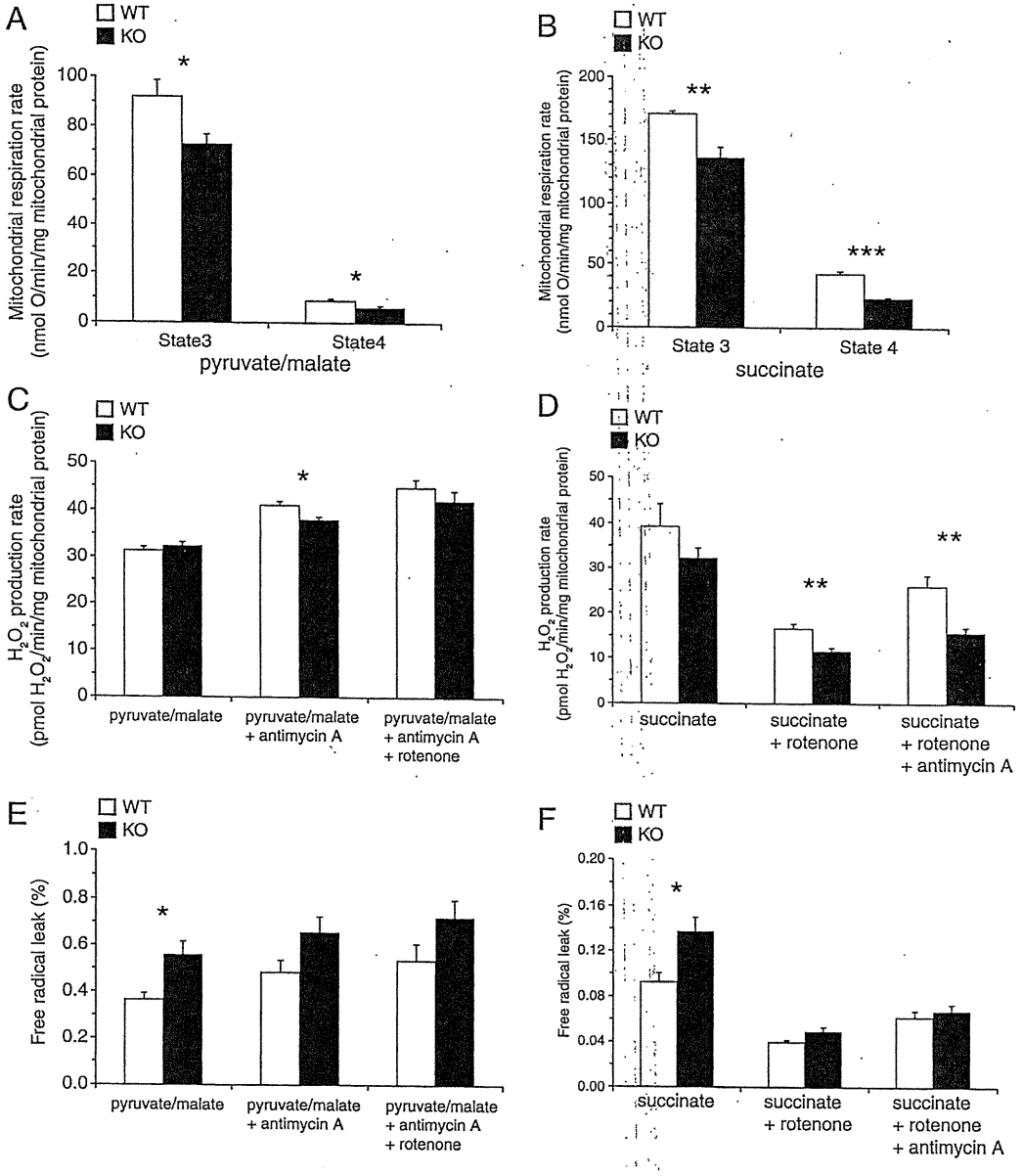

Fig. 4. Oxygen consumption rate and H_2O_2 production rate of mitochondria isolated from PINK1$^{+/+}$ and $^{-/-}$ MEFs. Open bars, PINK1$^{+/+}$ MEFs; closed bars, PINK1$^{-/-}$ MEFs. (A) State 3 and State 4 respiration rate of mitochondria with pyruvate/malate as a respiratory substrate. (B) State 3 and State 4 respiration rate of mitochondria with succinate as a respiratory substrate. Data were derived from the results of modular kinetic analysis (Fig. 3). State 3 respiration rates were the kinetic start points of the $\Delta\psi$-consumers (the sum of the phosphorylating system and proton leak). State 4 respiration rates were average values of the respiration rates at the kinetic start points of substrate oxidation and proton leak. (C, D) Mitochondrial H_2O_2 production rate with pyruvate/malate (C) or succinate (D) as a respiratory substrate. (E, F) Percentage free radical leak (FRL) for State 4 respiration with pyruvate/malate (E) or succinate (F) as a respiratory substrate. Error bars indicate SEM ($n=5$ and 4 independent mitochondrial preparations for pyruvate/malate and succinate respiration, respectively). *$P<0.05$; **$P<0.01$; ***$P<0.001$.

which partially dissipates the membrane potential without ATP synthesis, was also not changed (Fig. 3B). Therefore, the decrease in membrane potential caused by loss of PINK1 is likely to have been caused only by lower activity of the $\Delta\psi$-producer, substrate oxidation (Fig. 3A). This is the first report showing that mitochondrial membrane potential decrease caused by loss of PINK1, which is the key event for the following mitochondrial elimination, was not due to proton leak, but to respiratory chain defects. We used only succinate (a complex II-linked substrate) as a respiratory substrate in the modular kinetic analysis for technical reasons. However, complex I-linked respiration (pyruvate/malate) was also decreased in PINK1$^{-/-}$ MEFs like succinate respiration (Fig. 4A).

The mitochondrial respiration rates in State 4 were decreased in PINK1$^{-/-}$ MEFs, and consequently, the proportions of free radical leak were significantly higher in PINK1$^{-/-}$ MEFs than in PINK1$^{+/+}$ MEFs (Figs. 4E and F). Because the differences disappeared with addition of rotenone (complex I inhibitor, which inhibits reverse electron flow from coenzyme Q to complex I), ROS generation enhanced by loss of PINK1 was mostly from complex I. These results are partially consistent with those in previous reports, suggesting that MPTP and rotenone induce neuronal cell death by inhibiting complex I activity, leading to a PD-like phenotype (Dauer and Przedborski, 2003; Jackson-Lewis and Przedborski, 2007; Trojanowski, 2003).

In this study, we developed an *in vitro* PD model, the PINK1$^{-/-}$ MEF line, and established the experimental conditions for cell growth to detect mitochondrial dysfunction. This is the first report showing that complete ablation of PINK1 causes a decrease in mitochondrial membrane potential, which is not due to proton leak, but to respiratory chain defects.

Supplementary materials related to this article can be found online at doi:10.1016/j.nbd.2010.08.027.

Acknowledgments

This work was supported by a Grant-in-Aid for Scientific Research for Young Scientists (B) from JSPS (T.A. and S.Saiki), a JSPS fellowship (T.A.), Nagao Memorial Fund (S. Saiki) and a Grant from Takeda Scientific Foundation (S. Saiki and T.A.). We thank Dr. Noriyuki Matsuda for assistance to obtain immortalized cells.

References

Abou-Sleiman, P.M., Muqit, M.M., Wood, N.W., 2006. Expanding insights of mitochondrial dysfunction in Parkinson's disease. Nat. Rev. Neurosci. 7, 207–219.

Amo, T., Brand, M.D., 2007. Were inefficient mitochondrial haplogroups selected during migrations of modern humans? A test using modular kinetic analysis of coupling in mitochondria from cybrid cell lines. Biochem. J. 404, 345–351.

Barja, G., Cadenas, S., Rojas, C., Pérez-Campo, R., López-Torres, M., 1994. Low mitochondrial free radical production per unit O_2 consumption can explain the simultaneous presence of high longevity and high aerobic metabolic rate in birds. Free Radic. Res. 21, 317–327.

Brand, M.D., 1990. The proton leak across the mitochondrial inner membrane. Biochim. Biophys. Acta 1018, 128–133.

Brand, M.D., 1995. Measurement of mitochondrial protonmotive force. In: Brown, G.C., Cooper, C.E. (Eds.), Bioenergetics, a practical approach. IRL Press, Oxford, pp. 39–62.

Brand, M.D., 1998. Top-down elasticity analysis and its application to energy metabolism in isolated mitochondria and intact cells. Mol. Cell. Biochem. 184, 13–20.

Brand, M.D., Chien, L.F., Diolez, P., 1994. Experimental discrimination between proton leak and redox slip during mitochondrial electron transport. Biochem. J. 297, 27–29.

Chu, C.T., 2010. Tickled PINK1: mitochondrial homeostasis and autophagy in recessive Parkinsonism. Biochim. Biophys. Acta 1802, 20–28.

Clark, I.E., Dodson, M.W., Jiang, C., Cao, J.H., Huh, J.R., Seol, J.H., Yoo, S.J., Hay, B.A., Guo, M., 2006. *Drosophila pink1* is required for mitochondrial function and interacts genetically with *parkin*. Nature 441, 1162–1166.

Dauer, W., Przedborski, S., 2003. Parkinson's disease: mechanisms and models. Neuron 39, 889–909.

Exner, N., Treske, B., Paquet, D., Holmstrom, K., Schiesling, C., Gispert, S., Carballo-Carbajal, I., Berg, D., Hoepken, H.H., Gasser, T., Krüger, R., Winklhofer, K.F., Vogel, F., Reichert, A.S., Auburger, G., Kahle, P.J., Schmid, B., Haass, C., 2007. Loss-of-function of human PINK1 results in mitochondrial pathology and can be rescued by parkin. J. Neurosci. 27, 12413–12418.

Gandhi, S., Wood-Kaczmar, A., Yao, Z., Plun-Favreau, H., Deas, E., Klupsch, K., Downward, J., Latchman, D.S., Tabrizi, S.J., Wood, N.W., Duchen, M.R., Abramov, A.Y., 2009. PINK1-associated Parkinson's disease is caused by neuronal vulnerability to calcium-induced cell death. Mol. Cell 33, 627–638.

Gautier, C.A., Kitada, T., Shen, J., 2008. Loss of PINK1 causes mitochondrial functional defects and increased sensitivity to oxidative stress. Proc. Natl. Acad. Sci. U. S. A. 105, 11364–11369.

Geisler, S., Holmström, K.M., Skujat, D., Fiesel, F.C., Rothfuss, O.C., Kahle, P.J., Springer, W., 2010. PINK1/Parkin-mediated mitophagy is dependent on VDAC1 and p62/SQSTM1. Nat. Cell Biol. 12, 119–131.

Gispert, S., Ricciardi, F., Kurz, A., Azizov, M., Hoepken, H.H., Becker, D., Voos, W., Leuner, K., Müller, W.E., Kudin, A.P., Kunz, W.S., Zimmermann, A., Roeper, J., Wenzel, D., Jendrach, M., García-Arencíbia, M., Fernández-Ruiz, J., Huber, L., Rohrer, H., Barrera, M., Reichert, A.S., Rüb, U., Chen, A., Nussbaum, R.L., Auburger, G., 2009. Parkinson phenotype in aged PINK1-deficient mice is accompanied by progressive mitochondrial dysfunction in absence of neurodegeneration. PLoS One 4, e5777.

Grünewald, A., Gegg, M.E., Taanman, J.W., King, R.H., Kock, N., Klein, C., Schapira, A.H., 2009. Differential effects of PINK1 nonsense and missense mutations on mitochondrial function and morphology. Exp. Neurol. 219, 266–273.

Haque, M.E., Thomas, K.J., D'Souza, C., Callaghan, S., Kitada, T., Slack, R.S., Fraser, P., Cookson, M.R., Tandon, A., Park, D.S., 2008. Cytoplasmic Pink1 activity protects neurons from dopaminergic neurotoxin MPTP. Proc. Natl. Acad. Sci. U. S. A. 105, 1716–1721.

Hofhaus, G., Johns, D.R., Hurko, O., Attardi, G., Chomyn, A., 1996. Respiration and growth defects in transmitochondrial cell lines carrying the 11778 mutation associated with Leber's hereditary optic neuropathy. J. Biol. Chem. 271, 13155–13161.

Jackson-Lewis, V., Przedborski, S., 2007. Protocol for the MPTP mouse model of Parkinson's disease. Nat. Protoc. 2, 141–151.

Kawajiri, S., Saiki, S., Sato, S., Sato, F., Hatano, T., Eguchi, H., Hattori, N., 2010. PINK1 is recruited to mitochondria with parkin and associates with LC3 in mitophagy. FEBS Lett. 584, 1073–1079.

Kim, Y., Park, J., Kim, S., Song, S., Kwon, S.K., Lee, S.H., Kitada, T., Kim, J.M., Chung, J., 2008. PINK1 controls mitochondrial localization of Parkin through direct phosphorylation. Biochem. Biophys. Res. Commun. 377, 975–980.

King, M.P., Attardi, G., 1989. Human cells lacking mtDNA: repopulation with exogenous mitochondria by complementation. Science 246, 500–503.

Lambert, A.J., Buckingham, J.A., Boysen, H.M., Brand, M.D., 2010. Low complex I content explains the low hydrogen peroxide production rate of heart mitochondria from the long-lived pigeon, Columba livia. Aging Cell 9, 78–91.

Liu, W., Vives-Bauza, C., Acin-Perez, R., Yamamoto, A., Tan, Y., Li, Y., Magrane, J., Stavarache, M.A., Shaffer, S., Chang, S., Kaplitt, M.G., Huang, X.Y., Beal, M.F., Manfredi, G., Li, C., 2009. PINK1 defect causes mitochondrial dysfunction, proteasomal deficit and alpha-synuclein aggregation in cell culture models of Parkinson's disease. PLoS One 4, e4597.

Matsuda, N., Sato, S., Shiba, K., Okatsu, K., Saisho, K., Gautier, C.A., Sou, Y.S., Saiki, S., Kawajiri, S., Sato, F., Kimura, M., Komatsu, M., Hattori, N., Tanaka, K., 2010. PINK1 stabilized by mitochondrial depolarization recruits Parkin to damaged mitochondria and activates latent Parkin for mitophagy. J. Cell Biol. 189, 211–221.

Narendra, D., Tanaka, A., Suen, D.F., Youle, R.J., 2008. Parkin is recruited selectively to impaired mitochondria and promotes their autophagy. J. Cell Biol. 183, 795–803.

Narendra, D.P., Jin, S.M., Tanaka, A., Suen, D.F., Gautier, C.A., Shen, J., Cookson, M.R., Youle, R.J., 2010. PINK1 is selectively stabilized on impaired mitochondria to activate Parkin. PLoS Biol. 8, e1000298.

Park, J., Lee, S.B., Lee, S., Kim, Y., Song, S., Kim, S., Bae, E., Kim, J., Shong, M., Kim, J.M., Chung, J., 2006. Mitochondrial dysfunction in *Drosophila PINK1* mutants is complemented by *parkin*. Nature 441, 1157–1161.

Pridgeon, J.W., Olzmann, J.A., Chin, L.S., Li, L., 2007. PINK1 protects against oxidative stress by phosphorylating mitochondrial chaperone TRAP1. PLoS Biol. 5, e172.

Reitzer, L.J., Wice, B.M., Kennell, D., 1979. Evidence that glutamine, not sugar, is the major energy source for cultured HeLa cells. J. Biol. Chem. 254, 2669–2676.

Reynafarje, B., Costa, L.E., Lehninger, A.L., 1985. O_2 solubility in aqueous media determined by a kinetic method. Anal. Biochem. 145, 406–418.

Sandebring, A., Thomas, K.J., Beilina, A., van der Brug, M., Cleland, M.M., Ahmad, R., Miller, D.W., Zambrano, I., Cowburn, R.F., Behbahani, H., Cedazo-Mínguez, A., Cookson, M.R., 2009. Mitochondrial alterations in PINK1 deficient cells are influenced by calcineurin-dependent dephosphorylation of dynamin-related protein 1. PLoS One 4, e5701.

Trojanowski, J.Q., 2003. Rotenone neurotoxicity: a new window on environmental causes of Parkinson's disease and related brain amyloidoses. Exp. Neurol. 179, 6–8.

Twig, G., Elorza, A., Molina, A.J., Mohamed, H., Wikstrom, J.D., Walzer, G., Stiles, L., Haigh, S.E., Katz, S., Las, G., Alroy, J., Wu, M., Py, B.F., Yuan, J., Deeney, J.T., Corkey, B. E., Shirihai, O.S., 2008. Fission and selective fusion govern mitochondrial segregation and elimination by autophagy. EMBO J. 27, 433–446.

Valente, E.M., Abou-Sleiman, P.M., Caputo, V., Muqit, M.M., Harvey, K., Gispert, S., Ali, Z., Del Turco, D., Bentivoglio, A.R., Healy, D.G., Albanese, A., Nussbaum, R., González-Maldonado, R., Deller, T., Salvi, S., Cortelli, P., Gilks, W.P., Latchman, D.S., Harvey, R.J., Dallapiccola, B., Auburger, G., Wood, N.W., 2004. Hereditary early-onset Parkinson's disease caused by mutations in *PINK1*. Science 304, 1158–1160.

Vives-Bauza, C., Zhou, C., Huang, Y., Cui, M., de Vries, R.L., Kim, J., May, J., Tocilescu, M.A., Liu, W., Ko, H.S., Magrane, J., Moore, D.J., Dawson, V.L., Grailhe, R., Dawson, T.M., Li, C., Tieu, K., Przedborski, S., 2010. PINK1-dependent recruitment of Parkin to mitochondria in mitophagy. Proc. Natl. Acad. Sci. U. S. A. 107, 378–383.

Wood-Kaczmar, A., Gandhi, S., Yao, Z., Abramov, A.Y., Miljan, E.A., Keen, G., Stanyer, L., Hargreaves, I., Klupsch, K., Deas, E., Downward, J., Mansfield, L., Jat, P., Taylor, J., Heales, S., Duchen, M.R., Latchman, D., Tabrizi, S.J., Wood, N.W., 2008. PINK1 is necessary for long term survival and mitochondrial function in human dopaminergic neurons. PLoS One 3, e2455.

Yang, Y., Ouyang, Y., Yang, L., Beal, M.F., McQuibban, A., Vogel, H., Lu, B., 2008. Pink1 regulates mitochondrial dynamics through interaction with the fission/fusion machinery. Proc. Natl. Acad. Sci. U. S. A. 105, 7070–7075.

Phenotype of the 202 Adenine Deletion in the *parkin* Gene: 40 Years of Follow-Up

Sharon Hassin-Baer, MD,[1,2] Nobutaka Hattori, MD, PhD,[3] Oren S. Cohen, MD,[1,2] Magdalena Massarwa, MD,[1] Simon D. Israeli-Korn, MA, MRCP (UK),[1] and Rivka Inzelberg, MD[1,2*]

[1]*The Sagol Neuroscience Center, Department of Neurology, Sheba Medical Center, Tel Hashomer, Israel;* [2]*Sackler Faculty of Medicine, Tel Aviv University, Tel Aviv, Israel;* [3]*Department of Neurology, Juntendo University Medical School, Tokyo, Japan*

ABSTRACT

Background: We describe the four decades follow-up of 14 *parkin* patients belonging to two large eight-generation-long in-bred Muslim-Arab kindreds.

Results: All patients had a single base-pair of adenine deletion at nucleotide 202 of exon 2 (202A) of the *parkin* gene (all homozygous, one heterozygous). Parkinson's disease onset age was 17–68 years. Special features were intractable axial symptoms (low back pain, scoliosis, camptocormia, antecollis), postural tremor, and preserved cognition.

Conclusions: The 202A deletion of the *parkin* gene causes early-onset Parkinson's disease with marked levodopa/STN-DBS–resistant axial features. Postural tremor and preserved cognition, even after 40 years of disease, were also evident. © 2011 *Movement* Disorder Society

Key Words: Parkinson's disease; genetics; Parkin; PARK2; follow-up

Introduction

Mutations in the *parkin* gene (6q25.2-6q27, MIM 602544) are the most common cause of monogenic autosomal recessive Parkinson's disease (PD).[1,2] The phenotype includes early onset of classic PD symptoms, but may vary with respect to additional atypical features.[3–5] Exonic deletions or multiplications and truncating or missense mutations have been described.[1–6] No reports point to ethnic clusters of specific *parkin* mutations. We describe four-decades follow-up of 14 *parkin* patients belonging to two large in-bred Muslim-Arab kindreds.

Methods

PD patients of Arabic-origin with age of disease onset < 50 years were recruited from the Sheba Medical Center Movement Disorders Clinic. The Institutional Review Board approved the use of human subjects for this study. All patients and family members signed informed consent for participating in the study.

Participants were examined by a movement disorders specialist at 2–12 months intervals. Asymptomatic family members were examined once at the time of DNA collection. DNA was extracted from blood leukocytes. All exons of the *parkin* gene were screened for deletions, insertions, or point mutations by direct sequencing of the PCR products, sequenced on both strands as previously described.[4]

Results

Thirteen of 14 PD patients and 15 family members consented to genetic testing. Patient characteristics are summarized in Table 1 (10 men, 4 women; mean age 52 ± 10 years; range 35–73 years).

In all 13 patients, the same *parkin* mutation was found: a single base-pair deletion of adenine at nucleotide 202 of exon 2 (202A), causing an out-frame mutation with an early-stop codon (12 homozygous, 1 heterozygous) and one patient was not genotyped. The mutant *parkin* lacks a part of the Ubl domain and the entire region of the RING box, suggesting loss of activity of E3.

Phenotype and Clinical Course

All patients belong to two large Muslim-Arab in-bred *hamulas* (kindreds). Each *hamula* can trace their ancestry to a few founders about eight generations ago. Family A traced back five generations and divided into three branches shown as Aa, Ab, and Ac Family B traced back eight generations.

Mean age ± SD at PD onset was 31 ± 15 years (range 17–68) and disease duration 21 ± 13 (median 19, range 1–41 years) (Table 1). The first patient (B-VII-22) was seen in our clinic in 1963, aged 27 years. She complained of "bent trunk" and slowing since the age of 23. Her first cousin (B-VII-25) was examined in 1989, aged 19 years due to scolisois and

***Correspondence to:** Dr. Rivka Inzelberg, The Sagol Neuroscience Center, Department of Neurology, Sheba Medical Center, Tel Hashomer, 52621, Israel; inzelber@post.tau.ac.il.

Relevant conflicts of interest/financial disclosures: Nothing to report. Full financial disclosures and author roles may be found in the online version of this article.

Received: 11 July 2010; **Revised:** 31 August 2010; **Accepted:** 3 September 2010
Published online 21 January 2011 in Wiley Online Library (wileyonlinelibrary.com). DOI: 10.1002/mds.23456

Table 1. Demographic characteristics and motor features of Parkinson's disease (PD) patients with the *parkin* 202A deletion

Patient No.	*Parkin* 202A deletion	Gender	Age	Age of onset	PD duration	H&Y stage	Presenting sign	Rest tremor	Rig.	Asym	Brad.	Post. Inst.	Gait dist.	Post. tremor
Aa-II-3	HOM	M	58	17	41	3	Hand tremor	+	+	+	+	+	+	+
Aa-II-8	HOM	M	50	15	35	4	Leg dystonia	+	+	+	+	+	+	+
Aa-II-10	HOM	F	48	47	1	2	Leg tremor		+	+	+		+	
Aa-II-11	HOM	M	47	30	17	3	Leg tremor	+	+	+	+	+	+	+
Ab-IV-14	NG	M	73	68	5	3	Slow gait	+	+	+	+	+	+	
Ab-V-7	HOM	F	47	18	29	3	Hand tremor	+	+	+		+	+	+
Ac-IV-5	HOM	F	35	17	18	4	Hand tremor	+	+	+	+	+	+	+
B-VII-8	HOM	M	62	35	27	4	Leg tremor	+	+	+	+			+
B-VII-10	HOM	M	59	28	31	4	Hand tremor	+	+	+	+	+	+	+
B-VII-13	HOM	M	49	37	12	3	Leg tremor	+	+	+	+			+
B-VII-17	HOM	M	44	30	14	3	Hand tremor	+	+	+	+			+
B-VII-22	HOM	F	63	23	40	3	Camptocormia	+	+	+	+	+	+	+
B-VII-25	HOM	M	39	19	20	3	Hand tremor	+	+	+	+		+	+
Aa-II-6	HET	M	55	49	6	2	Hand tremor		+	+	+			
Mean±SD			52±10	31±15	21±13									

HET, heterozygous; HOM, homozygous; NG, not genotyped; Rig, rigidity; Asym, asymmetry; Brad, bradykinesia; Post Inst, postural instability; Dist, disturbance; Post, postural.

bradykinesia. The diagnosis of juvenile-onset PD was made in both.

The presenting symptom was hand tremor (n = 6), leg tremor (n = 4), foot dystonia (n = 1), camptocormia (n = 1), and gait disturbances (n = 1). Bradykinesia and rigidity were present in all patients and rest tremor in all but one. Eleven had postural hand tremor, three limb dystonia (two at PD onset) and three reported sleep benefit (Table 1).

Atypical motor features included prominent levodopa-resistant axial symptoms (n = 10): recurrent falls at onset (n = 1), gait disturbances at onset (n = 1), scoliosis (n = 1), camptocormia (progressive to fixed 90° trunk flexion, n = 2), antecollis (n = 1), lower back pain (LBP) (n = 8) (Table 2). Camptocormia and antecollis 5 years after onset were observed in a heterozygous carrier with an intermediate PD phenotype (onset 49 years) and very slow disease progression.

Pain was a predominant symptom (painful dystonia = 2, LBP = 8). Two patients manifested autonomic dysfuntion with complaints of constipation (Table 1).

None of the patients developed significant cognitive impairment or dementia during follow-up of up to 40 years (median 19 years). Seven patients had depressive symptoms but none develeoped hallucinosis or psychosis.

Response to Treatment and Progression

Levodopa response was excellent for appendicular signs but only minor for axial signs. All patients devel-

Table 2. Nonmotor/atypical features and therapy-related features of Parkinson's disease (PD) patients with the *parkin* 202A deletion

Patient No.	Psych.	Cognitive decline	Sleep benefit	Autonomic features	Additional axial features	Response to levodopa	Wearing off	Levodopa induced dyskinesia	UPDRS III (on/off)	DBS (Yr after PD onset)
Aa-II-3		–				+	+	+	52	
Aa-II-8	DEP	–	+			+	+	+	20/27	+ (30)
Aa-II-10		–	+	constip	LBP	NA	NA	NA	17/NA	
Aa-II-11		–				+			46	
Ab-IV-14		–		constip		+	+		38/41	
Ab-V-7	DEP	–	+		LBP	+	+	+	14	
Ac-IV-5	DEP	–				+	+	+	48/61	+ (14)
B-VII-8	DEP	–			LBP	+	+	+	16/22	
B-VII-10	DEP	–			LBP	+	+	+	37/64	+ (26)
B-VII-13	DEP	–			LBP	+	+		4/20	
B-VII-17		–			LBP	+	+		20/30	
B-VII-22	DEP	–			Camptocormia, LBP	+	+	+	37/48	
B-VII-25		–			Scoliosis, LBP	+	+	+	16/28	
Aa-II-6		–			Antecollis, Camptocormia	NA	NA	NA	NA	

DEP, depression; constip, constipation; LBP, Lower back pain; NA, not applicable.